The Domain Movement of an Enzyme Molecule Induced by Substrate Binding

Doctoral Thesis

January 2000

Jun Ishijima

Department of Biology, Graduate school of science

Osaka University

Contents

Abbreviations

AspAT	aspartate aminotransferase
AroAT	aromatic amino acid aminotransferase
PLP	pyridoxal 5'-phosphate
PMP	pyridoxamine 5'-phosphate
PDB	Protein Data Bank
Cn substrates	aliphatic amino acids with linear side chains $[CH_3(CH_2)_{n-3}C_{(\alpha)}H(NH_3^+)COO^-]$
Cn-PLP	aliphatic amino acid of n carbon atoms covalently bound to PLP by reduction with $NaBH_4$
Cn-PLP complex	*E. coli* AspAT complexed with Cn-PLP
2MeAsp	2-methylaspartate
Asp-PLP	aspartic acid covalently bound to PLP by reduction with $NaBH_4$

Abstract

Domain movement is sometimes essential for substrate recognition by an enzyme. X-ray crystallography of aminotransferase with a series of aliphatic substrates showed that the domain movement of aspartate aminotransferase was changed dramatically from an open to a closed form by the addition of only one CH_2 to the side chain of the C4 substrate $CH_3(CH_2)C_{(\alpha)}H(NH_3^+)COO^-$. These crystallographic results and reaction kinetics (Kawaguchi, S. *et al.* (1997) *J. Biochem. (Tokyo)* **122**, 55-63; Kawaguchi, S. and Kuramitsu, S. (1998) *J. Biol. Chem.* **273**, 18353-18364) enabled to estimate the free energy required for the domain movement.

Introduction

Induced-fit movement

The induced fit movement of an enzyme molecule upon the binding of substrate has been characterized for many enzymes, and is essential for catalysis. These phenomena are explained by Koshland's earlier idea (Koshland, 1958), in which the binding of substrate to an enzyme causes conformational changes that align the catalytic groups in their correct orientations. Since the unbound molecule takes multiple conformation, the induced-fit mechanism mediates against catalysis by increasing K_M without a corresponding increase in k_{cat}, compared with all the enzyme being in the active form in the absence of substrate (Fersht, 1985). Although the K_M value of the enzyme was increased, this conformational fluctuation constitutes a considerable advantage for association and dissociation of the substrate. The large conformational change is domain movement.

Domain movement of such enzymes (for example see Table I) can drastically change their active site environment from hydrophilic to hydrophobic, and such closure allows the enzymes to undergo reactions that are difficult in the aqueous phase. In order to elucidate the detailed mechanism of a given enzyme, it is necessary to estimate quantitatively the

Table I. Molecular movement of proteins.

Enzyme	Movement[a] (angstrom)	Reference
Domain Movement		
Formate Dehydrogenase	5.5	Lamzin *et al.*, 1994
Citrate Synthase	10	Remington *et al.*, 1982
c-Src tyrosine kinase	12	Xu *et al.*, 1997
Recoverin	14	Ames *et al.*, 1997
Tomato Bushy Stunt Virus Coat Protein	14	Olson *et al.*, 1983
Phosphoglycerate Kinase	27	Bernstein *et al.*, 1987
Calmodulin	60	Meador *et al.*, 1993
Diphtheria Toxin	65	Bennett *et al.*, 1994
Movement of Small Fragment		
Yersinia Protein Tyrosine Phosphatase	6	Stuckey *et al.*, 1994
Enolase	7	Lebioda and Stec, 1991
HIV-1 protease	7	Fitzgerald *et al.*, 1990
Triose Phosphate Isomerase (TIM)	7	Wierenga *et al.*, 1991
Malate Dehydrogenase (MDH)	8	Birktoft *et al.*, 1989
Immunoglobulin (CDR motion)	9	Rini *et al.*, 1992
Ras Protein	10	Pai *et al.*, 1990
Lactate Dehydrogenase (LDH)	11	Gerstein *et al.*, 1991
Triglyceride Lipase	12	Derewenda *et al.*, 1992
Annexin V (Trp motion)	18	Concha *et al.*, 1993
*Hha*I Methyltransferase	25	Cheng *et al.*, 1993

[a]Data from Gerstein *et al.* (1998)

energy required for domain movement. For the last two decades, molecular dynamic calculations have been used to predict the domain movement of enzymes (Karplus & McCammon, 1983; Pugmire *et al.*, 1998). Recent studies indicate that single molecule measurements may also be useful in determining the energy required for domain fluctuation (Radmacher *et al.*, 1994; Mehta *et al.*, 1999). In spite of these trials, it has generally proven difficult to confirm quantitatively the free energy required for domain movement of an enzyme. In this study, I estimated the energy required for domain movement by analyzing the reactions of two aminotransferases with a series of aliphatic α-amino acid substrates.

Aminotransferases

Escherichia coli aspartate aminotransferase [EC 2.6.1.1] (AspAT) with the bound coenzyme pyridoxal 5'-phosphate (PLP) reacts with an α-amino acid to form the pyridoxamine 5'-phosphate (PMP) form of the enzyme and the α-keto acid (Kiick & Cook, 1983; Christen & Metzler, eds., 1985; Smith *et al.*, 1989; Kuramitsu *et al.*, 1990; Jäger *et al.*, 1994; Okamoto *et al.*, 1994):

$$\text{E-PLP} + \alpha\text{-amino acid} \rightleftarrows \text{E-PMP} + \alpha\text{-keto acid} \qquad (1).$$

AspAT is a unique "dual-substrate" enzyme that catalyzes this reaction for both acidic and hydrophobic amino acids (Kawaguchi *et al.*, 1997; Kawaguchi & Kuramitsu, 1998). In the catalytic mechanism, the catalytic group Lys258 is commonly used for both types of substrate. Arg386 is also frequently used for recognition of the α-carboxyl group of both types of substrate.

With acidic substrates, AspAT undergoes a large domain movement (Fig. 1). Arg292* (* indicates the residue supplied by the other subunit of the dimer.) moves from the outside to the inside of the active site with its accompanying water molecules and recognizes the ω-carboxyl group of the substrate (Christen & Metzler, eds., 1985; Smith *et al.*, 1989; Jäger *et al.*, 1994; Okamoto *et al.*, 1994). (Fig. 2).

With hydrophobic substrates, it is known that the catalytic efficiency increases in proportion to the side chain length of a series of straight aliphatic substrates (Cn substrates: Fig. 3) (Kawaguchi *et al.*, 1997; Kawaguchi & Kuramitsu, 1998). Surprisingly, consecutive additions of a single methylene group to the substrate (from C4 to C7) produce a constant effect on the stabilization energy of the transition state ($ES^{\ddagger}$) relative to the unbound state (E+S) (Kawaguchi *et al.*, 1997; Kawaguchi & Kuramitsu, 1998; see Fig. 5). The energy contribution of one methylene group in the alkyl chain to AspAT is –0.65 kcal mol^{-1} for longer hydrophobic substrates

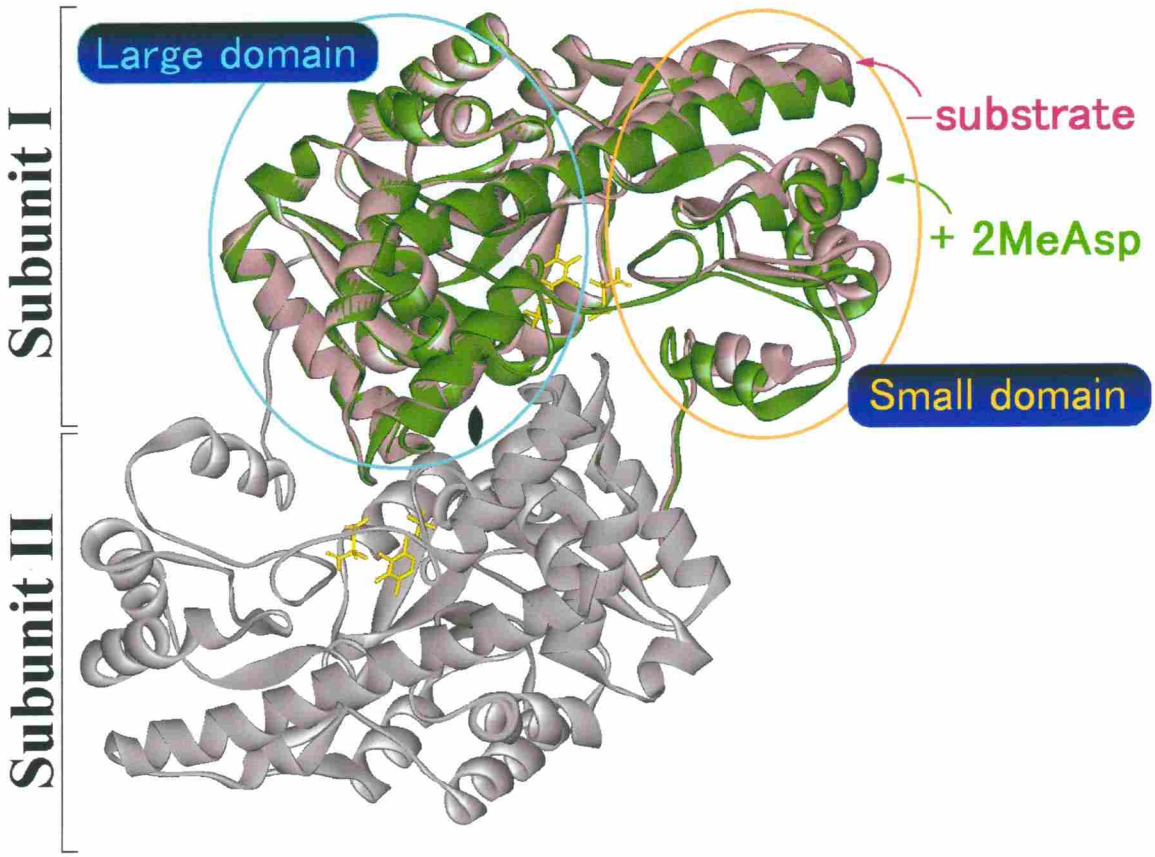

Fig. 1. Domain movement of *E. coli* AspAT on binding of 2-methylaspartate.
AspAT is a dimer with identical subunits I (colored pink or green) and II (colored gray). The large domain of subunit I without substrate (PDB code 1ARS (Okamoto *et al,* 1994)) (pink) was superimposed onto that complexed with 2-methylaspartate (PDB code 1ART (Okamoto *et al,* 1994)) (green). AspAT undergoes a domain movement when it binds to acidic substrates. This figure was produced using WebLab ViewerLite (MSI).

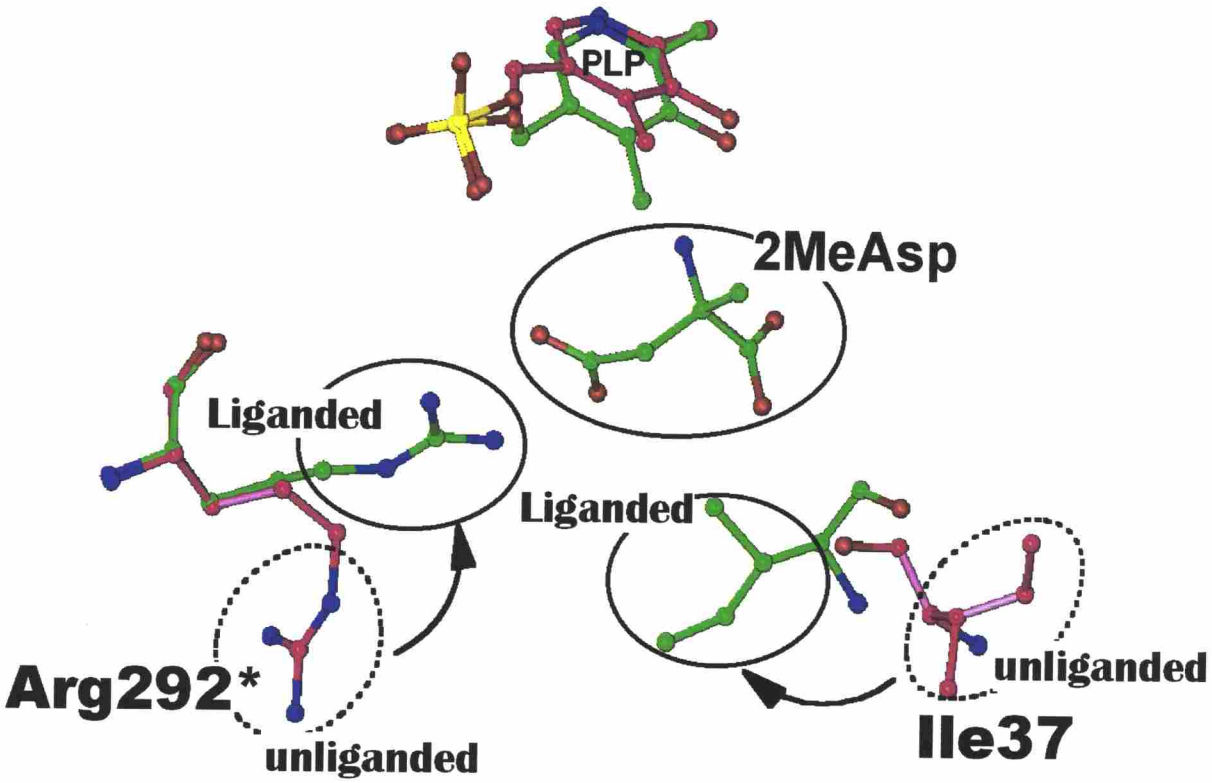

Fig. 2. The movement of Arg292 and Ile37 of *E. coli* AspAT on binding of 2-methylaspartate.

The structure of the unliganded PLP form (magenta) and 2-methylaspartate complex (green) (PDB code 1ARS and 1ART (Okamoto *et al,* 1994)). The side-chain orientation of Ile37 and Arg292* (* indicates the residue supplied by another subunit of the dimer) changes drastically depending on substrate binding. This figure was produced using program O (Jones *et al.*, 1991).

with C ≥ 5. Similar phenomena have been reported for many enzymes (Dorovska *et al.*, 1972; Ryu & Dordick, 1992; Wangikar *et al.*, 1995; Oue *et al.*, 1997). The energetic contribution of one methylene group in the substrate is 0.3 kcal mol^{-1} for horseradish peroxidase (Ryu & Dordick, 1992), –0.4 kcal mol^{-1} for *Bacillus amyloliquefaciens* subtilisin (Wangikar *et al.*, 1995), –0.9 kcal mol^{-1} for *Paracoccus denitrificans* AroAT (Oue *et al.*, 1997), and –1.5 kcal mol^{-1} for bovine α–chymotrypsin (Dorovska *et al.*, 1972) (see Fig. 13). This apparent uniformity of the substrate-binding site will be achieved by fluctuation of the enzyme molecule. Therefore, the linear correlation of the free energy with the chain length (from C5 to C7) of the substrate for AspAT (Fig. 12) suggests an apparently uniform hydrophobic environment of the substrate-binding pocket of this enzyme.

In this study, the three-dimensional structures of AspAT complexed with a series of straight-chain aliphatic amino acids were determined. With hydrophobic substrates with 3 (alanine) or 4 (2-amino butyric acid) carbon atoms, Arg292* remained outside the active site, as expected from the previous results with other hydrophobic substrates (Malashkevich *et al.*, 1995; Kawaguchi *et al.*, 1997; Okamoto *et al.*, 1999). Surprisingly, the positively charged ε-amino group of Arg292* moved into the active site on binding of hydrophobic substrates with C ≥ 5. Domain closure was also observed, as with acidic substrates. A detailed analysis of these structural

and kinetic results enabled to estimate the free energy required for domain movement. The energy thus obtained seems to explain the phenomena implied by single molecule measurements.

Experimental Procedures

Chemicals

A series of aliphatic α-amino acids [$(CH_3(CH_2)_{n-3}C_{(\alpha)}H(NH_3^+)COO^-$, n = 3 to 6] were covalently bound to PLP with $NaBH_4$ as a reducing agent (Figs. 3 and 4). These PLP-amino acids (Cn-PLP, n = 3 to 6) were purified on a DOWEX 1-X8 column (Dow Chemical). The structure of each product was confirmed by atomic composition, electrospray ionization mass spectrometry, and NMR. X-ray crystallography of the enzymes complexed with these substrate analogs (Protein Data Bank code 1C9C, 1CQ6, 1CQ7, and 1CQ8) also confirmed the structure of these compounds.

Protein Purification and Crystallization

AspAT purified as described previously (Kuramitsu *et al.*, 1990). It was then converted to the apoenzyme by adding 10 mM cysteine sulfinate and 0.5 M potassium phosphate (pH 8.0); excess PLP and cysteine sulfinate were removed using Sephadex G-50 gel filtration. The apoenzyme was converted to a holoenzyme by adding a 2-fold excess (with respect to enzyme concentration) of PLP-amino acid to the protein solution. Crystals of holoenzyme (Cn-PLP complex) were grown by the hanging drop/vapor diffusion method using ammonium sulfate as the precipitant.

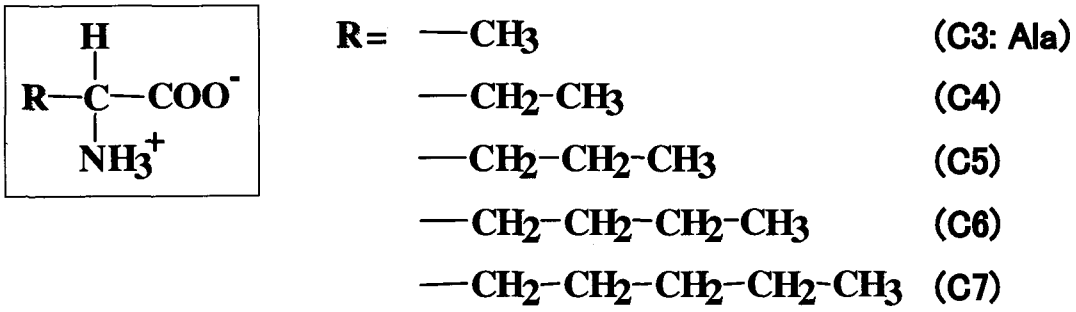

Fig. 3. Cn substrates

A series of aliphatic α-amino acid substrates (Cn substrates) used in this study.

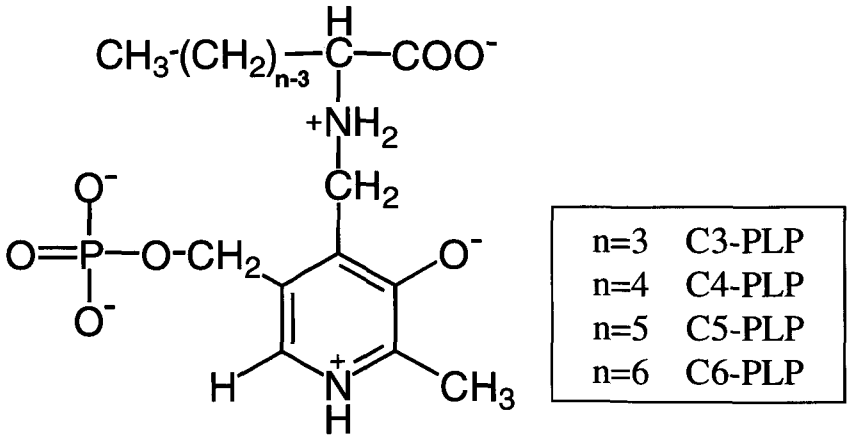

Fig. 4. Cn-PLP

A series of aliphatic α-amino acids were covalently bound to PLP with $NaBH_4$ as a reducing agent.

The 5 μl drops containing 40 mg ml^{-1} protein in 10 mM potassium phosphate, 10 μM PLP-amino acid, and 0.3 mM NaN_3 at pH 8.0 were mixed with an equal volume of reservoir solution that contained 35% saturated ammonium sulfate, 10 mM potassium phosphate, and 0.3 mM NaN_3 at pH 8.0, and then equilibrated against the reservoir solution at 20 °C. After 4 days, the drop was seeded with a small crystal obtained beforehand. The crystals reached their maximal size of 0.7 x 0.2 x 0.04 mm (C5-PLP complex) in 2-3 weeks.

Structure Determination by X-ray Crystallography

The diffraction data sets were collected with an R-AXIS IIc imaging plate detector (Rigaku), mounted on an RU-200 rotating anode generator (Rigaku), which was operated at 40 kV and 100 mA with monochromatized Cu*K*α radiation at room temperature. All the data were processed and scaled using the programs DENZO and SCALEPACK (Otwinowski, 1993). The conditions for data collection are summarized in Table II. The structures were determined by molecular replacement methods using the structure of the PLP form (PDB code 1ARS) or the PMP form (PDB code 1AMQ) as the starting model. Model refinement was performed by the CCP4 program suite (Collaborative Computational Project, Number 4, 1994) version 3.51, X-PLOR (Brünger, 1993) version 3.851, and program O (Jones *et al.*, 1991) version 6.2.2.

Table II. Crystallographic parameters

Analogs	C3-PLP[a]	C4-PLP	C5-PLP	C6-PLP
Space group	$C222_1$	$C222_1$	$C222_1$	$C222_1$
Cell constant (Å)				
a	156.98	157.15	157.58	157.72
b	87.27	86.32	85.59	85.57
c	79.73	79.24	78.92	78.79
Measured reflections	77627	79877	91223	66489
Unique reflections	19863	14620	20972	20719
Completeness (%)	91.0	96.2	98.5	97.4
R_{merge} (%)[b]	7.7	8.7	9.6	9.1
Source	Cu$K\alpha$	Cu$K\alpha$	Cu$K\alpha$	Cu$K\alpha$
Refinement				
R_{factor} (%)	20.2	24.1	21.5	21.3
R_{free} (%)[c]	27.1	29.7	25.1	27.0
Resolution (Å)	10 - 2.4	10 - 2.7	10 - 2.4	10 - 2.4
Number of water	119	140	122	109
Enzyme form	open	open	closed	closed
Arg292	out	out	in	in
Ile37	out	out	in	in

[a]C3-PLP represents L-alanine covalently bound to pyridoxal 5'-phosphate by reduction with $NaBH_4$.

[b]$R_{merge} = \Sigma|I_{obs} - \langle I_{obs}\rangle| / \Sigma\langle I_{obs}\rangle$

[c]R_{free} was calculated against reflections, 10% of the total, that were not used in the refinements.

Kinetic Analysis

The half-transamination reactions of the PLP form of the enzymes were followed spectrophotometrically at 360 nm as described previously (Kuramitsu *et al.*, 1990). The reaction conditions used were 50 mM 2-[4-(2-hydroxyethyl)-1-piperazinyl]ethanesulfonic acid (HEPES), 100 mM KCl, and 10 μM ethylenediaminetetraacetic acid (EDTA), pH 8.0, at 25 °C.

The kinetic parameters were determined using the following scheme (2) and Eq. (3).

$$E + S \underset{}{\overset{K_d}{\rightleftharpoons}} E \bullet S \xrightarrow[(ES^{\ddagger})]{k_{max}} E + P \qquad (2)$$

$$k_{app} = k_{max}[S] / (K_d + [S]) \qquad (3),$$

where E is the enzyme, S the substrate, E • S the enzyme–substrate complex, $ES^{\ddagger}$ the transition state, P the product, K_d the dissociation constant of E • S to E + S, k_{max} the maximum rate constant of the conversion of E • S into E + P, and k_{app} the apparent rate constant at a given substrate concentration. When the reaction condition is $[S] << K_d$ and the k_{app} value was directly proportional to the substrate concentration, Eq. (4), instead of Eq. (3), was used to determine the catalytic efficiency, k_{max} / K_d (Kuramitsu *et al.*, 1990):

$$k_{app} = (k_{max} / K_d)[S] \qquad (4)$$

The free energy difference between E + S and $ES^{\ddagger}$ ($\Delta G_T^{\ddagger}$) was calculated from Eq. (5) (Fig. 5).

$$\Delta G_T^{\ddagger} = RT(\ln(k_B T/h) - \ln(k_{max}/K_d)) \qquad (5)$$

where R is the gas constant, T the absolute temperature, k_B the Boltzmann constant, and h the Planck constant (Kuramitsu *et al.*, 1990).

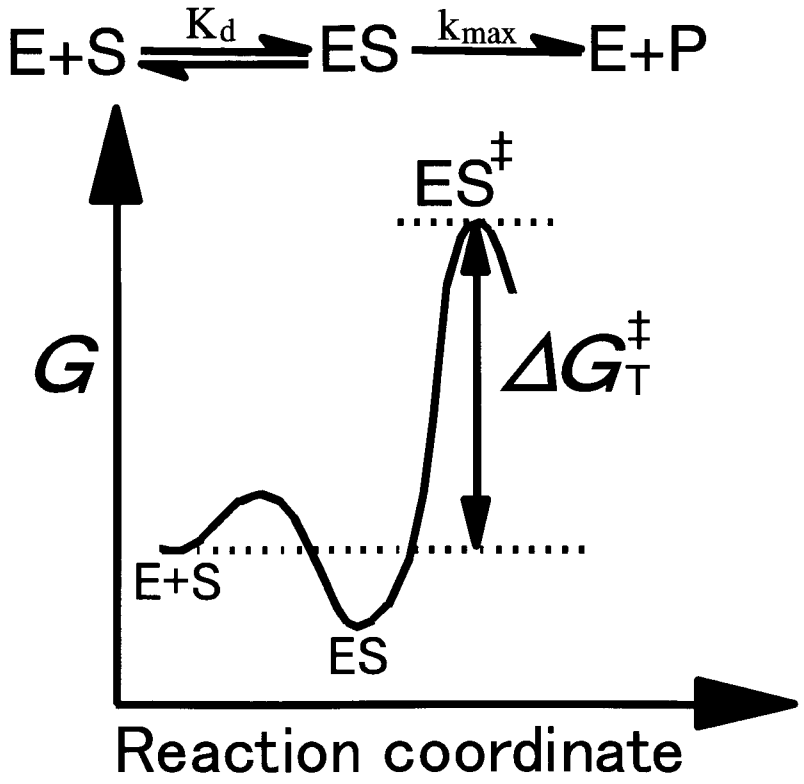

Fig. 5. Free energy diagram of enzymatic reaction.

Site-directed Mutagenesis

(1) Introduction of Cysteine Residue

The DTNB-titratable syncatalytic Cys390 (Birchmeier, 1973; Christen & Metzler, eds., 1985) was introduced into *E. coli* AspAT by three-primer polymerase chain reaction (PCR)-available site-directed mutagenesis. In the first PCR, the 192 bp fragment containing the mutation site was amplified as follows. The plasmid pKDHE19 (Kamitori *et al.*, 1987) which carries the *aspC* gene was denatured at 98 °C for 2 min in the PCR reaction mixture (with primers 5'-CTTCTGGTCGCGTTAACGTGT-GCGGGATGACACC-3' and 5'-GACGTTGTAAAACGACGGCCAG-3') without DNA polymerase. After the addition of KOD DNA polymerase (TOYOBO), 25 PCR cycles of 15 sec at 98 °C, 5 sec at 65 °C, and 30 sec at 74 °C were performed. In the second PCR, the above amplified 192 bp DNA fragment and the oligonucleotide 5'-AATGAAACCACCAAACT-TTACCTAGGCATTGACGGCATC-3' were used as PCR primers, and the 1129 bp DNA fragment was amplified by the same method as described above. This amplified fragment carrying the mutation site was cut by restriction endonucleases *Eco*RI and *Bst*PI, and was replaced by the corresponding fragment of the wild type *aspC* gene in the pKDHE19 plasmid (Kamitori *et al.*, 1987).

(2) Mutation of Ile37

The substitution of Ile37 with Gly, Ala, Val, and Met was performed by polymerase chain reaction (PCR)-available site-directed mutagenesis. The oligonucleotides containing mixed-base (5'-TTAACCTCGGGG(G/C)-TGGTGTATACAAAGATGAGACG-3' or 5'-TTAACCTCGGG(A/G/C)-(T/C)GGGTGTATACAAAGATGAGACG-3') and 5'-GACGTTGTAAA-ACGACGGCCAG-3' were used for PCR, and the 1218 bp DNA fragment was amplified by the same method as described above. This amplified fragment carrying the mutation site was cut by restriction endonucleases *Ava*I and *Mlu*I, and was replaced by the corresponding fragment of the wild type *aspC* gene in the pKDHE19 plasmid (Kamitori *et al.*, 1987).

The DNA sequence of these resultant plasmids was analyzed using an ABI PRISM 377 DNA sequencer (Perkin Elmer). No mutation was observed except for the designed mutation site.

Titration of SH Groups of the Enzymes

The reactivity of the SH groups in the enzymes was monitored with 5,5-dithiobis(2-nitrobenzoic acid) (DTNB) at 412 nm and 25 °C by a method similar to that described previously (Kuramitsu *et al.*, 1981). The enzyme concentration used was about 0.5 mg ml^{-1}. The buffer used contained 50 mM HEPES, 100 mM KCl, and 10 μM EDTA at pH 8.0.

Results

Overall Structure of AspAT Complexes

In order to reveal the binding mode of the series of aliphatic amino acids (Cn substrates: $CH_3(CH_2)_{n-3}C_{(\alpha)}H$ $(NH_3^+)COO^-$, n = 3 to 7), the substrate analogs covalently bound to PLP (Cn-PLP, n = 3 to 6) were synthesized. The enzyme – Cn-PLP complexes prepared as described in "EXPERIMENTAL PROCEDURES" were crystallized, and their three-dimensional structures were determined (Table II and Figs. 6-10). The coordinates of these enzyme – Cn-PLP complexes have been deposited in the Research Collaboratory for Structural Bioinformatics Protein Data Bank. The accession numbers are 1C9C (C3-PLP complex), 1CQ6 (C4-PLP complex), 1CQ7 (C5-PLP complex), and 1CQ8 (C6-PLP complex).

Fig. 6 shows the overall structure of the Cn-PLP complexes. AspAT is a dimer with two identical subunits. Each subunit is composed of a large domain (amino acid residues 48-325) and a small domain (residues 5-47 and 326-405) (Christen & Metzler, eds., 1985; Jäger *et al.*, 1994; Okamoto *et al.*, 1994). In Fig. 6, the large domains of all the Cn-PLP complexes are superimposed. AspATs exhibit significant domain movement on substrate binding (Christen & Metzler, eds., 1985; Jäger *et al.*, 1994; Okamoto *et al.*, 1994). The small domain of *E. coli* AspAT

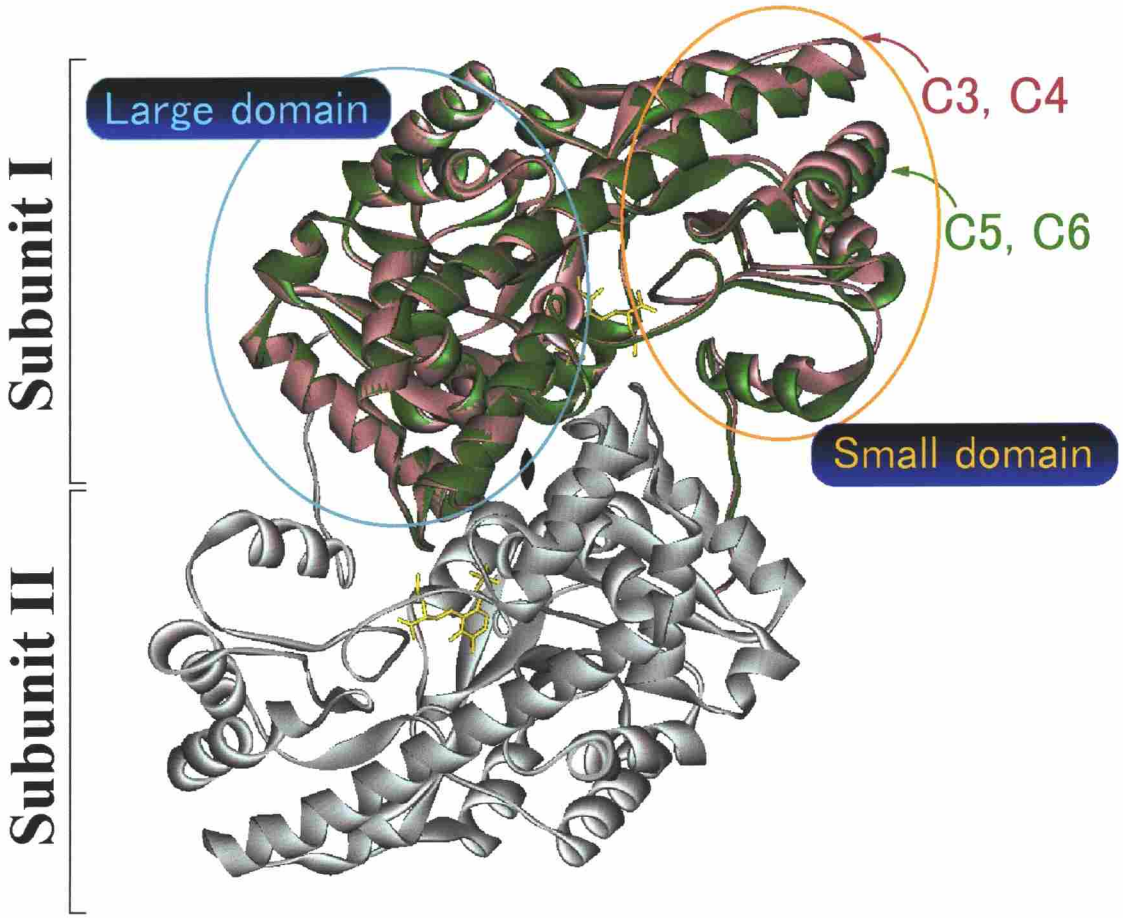

Fig. 6. The domain movement of AspAT upon binding of hydrophobic substrates. The large domain of subunit I complexed with C3-PLP or C4-PLP (pink) was superimposed onto that complexed with C5-PLP or C6-PLP (green). Although the complexes were crystallized under the same conditions, the C3-PLP or C4-PLP complex adopted the open-like form and the C5-PLP or C6-PLP complex adopted the closed-like form. The addition of only one CH_2 group to the C4-PLP complex induced domain closure in the C5-PLP complex. This figure was produced using WebLab ViewerLite (MSI).

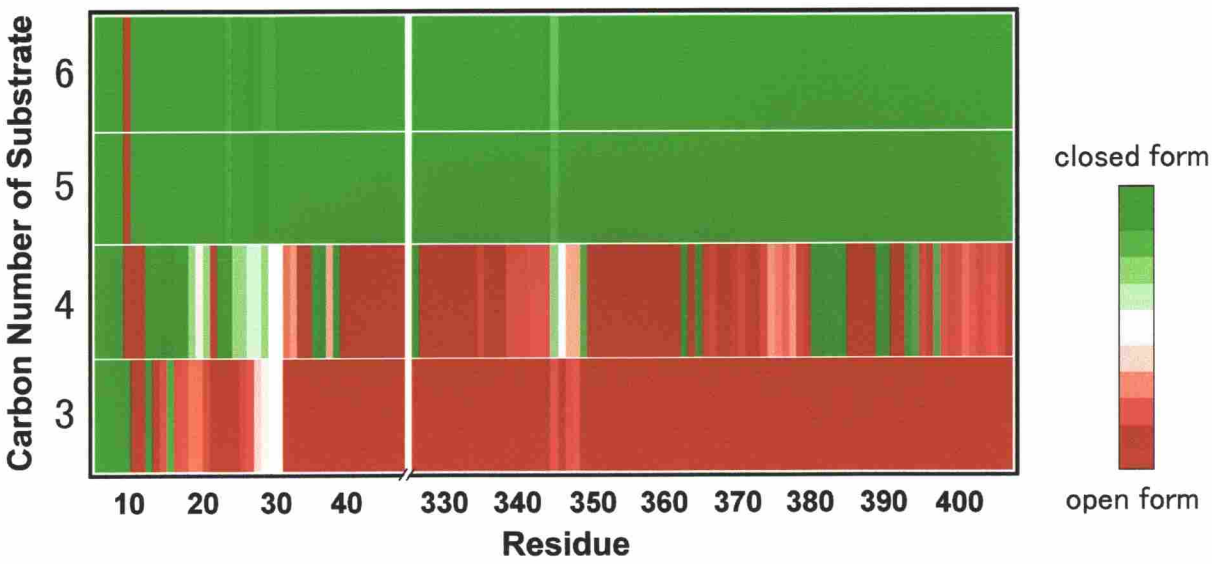

Fig. 7. The displacement of the C_α atoms in the small domain of AspAT upon binding of hydrophobic substrates.

The root-mean-square deviations of the C_α atoms in the small domain (residues 5-47 and 326-405) relative to the structure in the absence or presence of substrate (PDB code 1ARS or 1ART (Okamoto *et al.*, 1994)) were normalized and are represented by a color gradient. The color red indicates that the atomic coordinates of a C_α atom in the Cn-PLP complex are near those of the unliganded open form (PDB code 1ARS), and green indicates that the atomic coordinates are near those of the closed form complexed with an acidic substrate analog, 2-methylaspartate (PDB code 1ART). The color white indicates that an atom is more than 2 Å from either the open or closed form.

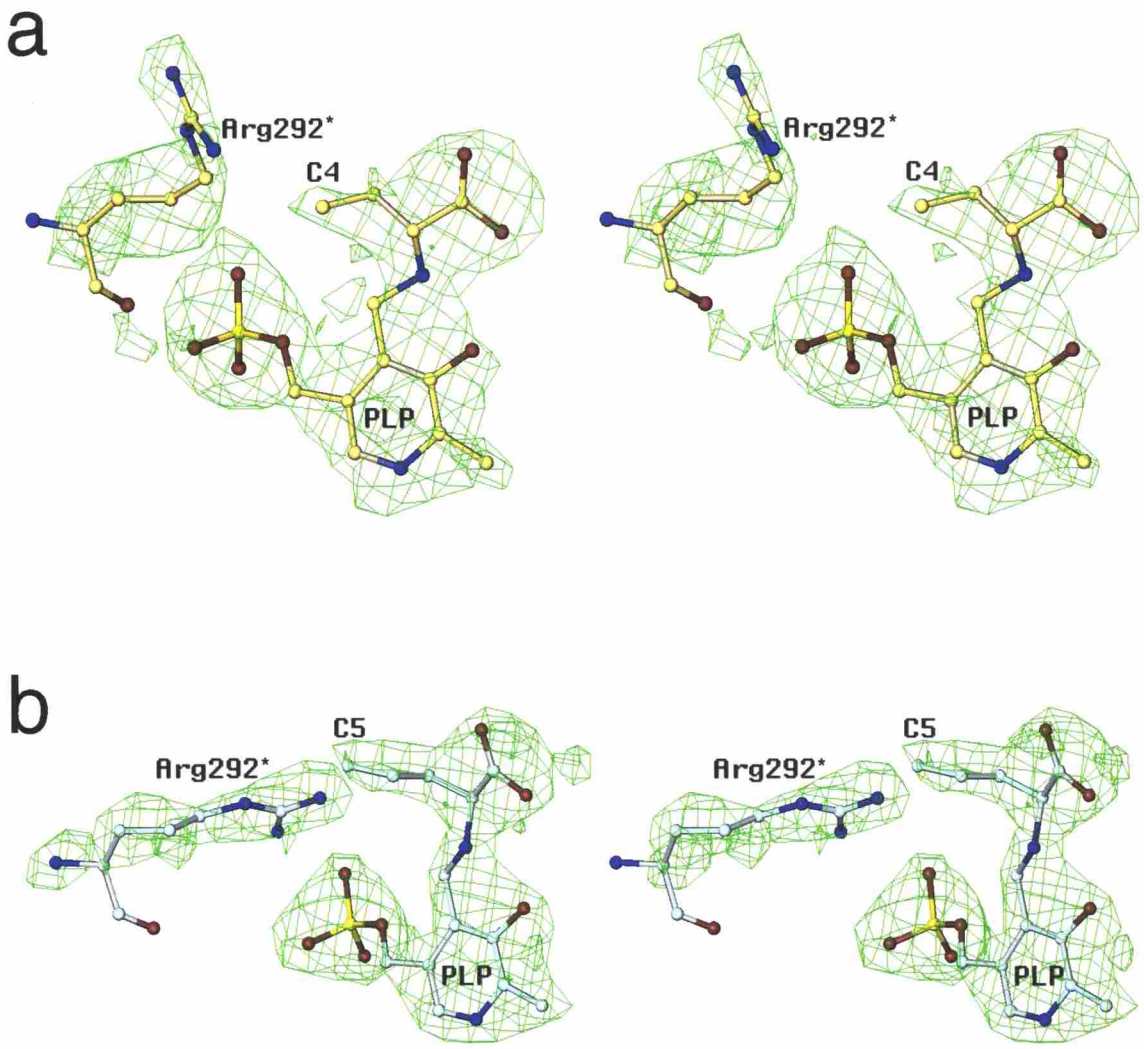

Fig. 8. Stereoviews of AspAT bound to substrate analogs.

Only Arg292* and the substrate analogs are indicated for clarity. a, the substrate analog is C4-PLP (the moiety of coenzyme is labeled as "PLP" and that of substrate as "C4"). The active-site conformation of the C4-PLP complex is almost identical to that of substrate-free AspAT (Jäger *et al.*, 1994; Okamoto *et al.*, 1994). b, the substrate analog is C5-PLP.

Each substrate analog and the side chain of Arg292* are superimposed onto the ($\mathbf{F}_o$ - $\mathbf{F}_c$) omit map contoured at 2.5 σ (a) and 3 σ (b) with these atoms omitted. These figures were produced using program O (Jones *et al.*, 1991).

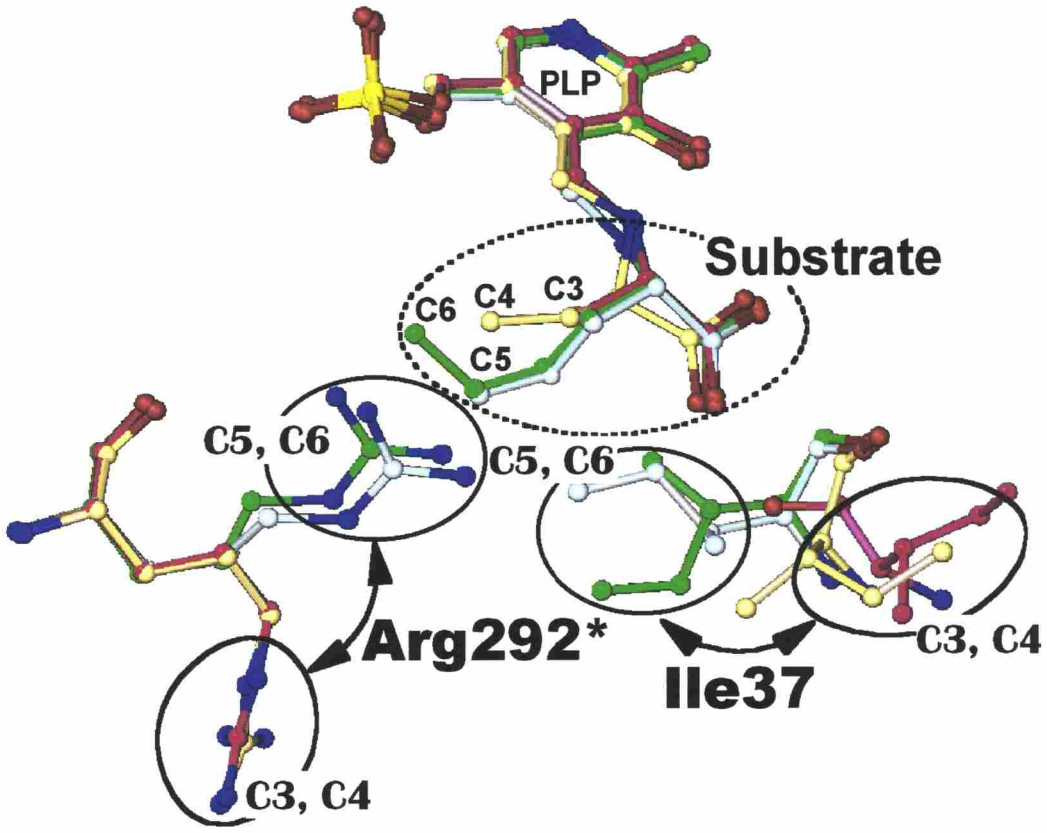

Fig. 9. Ile37 and Arg292 of AspAT bound to hydrophobic substrate analogs.
The structure of the C3-PLP complex (magenta), C4-PLP complex (yellow), C5-PLP complex (cyan), and C6-PLP complex (green). Note that the side-chain orientation of Arg292* changes drastically depending on substrate. This figure was produced using program O (Jones *et al.*, 1991).

rotates by 5-6° to form the closed form of the enzyme (Jäger *et al.*, 1994; Okamoto *et al.*, 1994) and this domain closure changes the active site environment by expelling bulk water molecules from the active site. The positions of the C_α atoms in the small domains of the C3-PLP and C4-PLP complexes (shown in pink) were almost identical to those of the "open form" without a bound substrate (Figs. 1 and 2) (PDB code 1ARS (Okamoto *et al.*, 1994)). In contrast to these analogs, the positions for the C5-PLP and C6-PLP complexes (green) were very close to those for the "closed form" complexed with 2-methylaspartate (PDB code 1ART (Okamoto *et al.*, 1994)), which is an acidic substrate analog with high affinity (Figs. 1 and 2). The root-mean-square deviations relative to C6-PLP were 0.980, 0.865, and 0.250 Å for the C3-PLP, C4-PLP, and C5-PLP complexes, respectively.

The root-mean-square deviations of each C_α atom between the open form (PDB code 1ARS) and the closed form (PDB code 1ART) (Okamoto *et al.*, 1994) were normalized and are shown by the color gradient in Fig. 7.

These observations indicate that the enzyme conformations differed markedly between the C4-PLP complex (open form) and the C5-PLP complex (closed form).

Movement of Arg292 in the Active Site

Figs. 8 show the electron density maps of the active sites for the C4-PLP and 5-PLP complexes, respectively. The C3-PLP to C6-PLP complexes are superimposed in Fig. 9. When C3-PLP or C4-PLP was bound to the enzyme (Figs. 8 and 9), the hydrophilic Arg292* was situated outside the cleft. This Arg292* is known to form salt bridges and hydrogen bonds with the ω-carboxyl group of bound aspartate or glutamate substrates (Fig. 2) (Christen & Metzler, eds., 1985; Kamitori *et al.*, 1990; Jäger *et al.*, 1994; Miyahara *et al.*, 1994; Okamoto *et al.*, 1994).

In spite of the absence of a negatively charged side chain in the substrate, the positively charged Arg292* moved into the active site when hydrophobic C5-PLP or C6-PLP was bound (Figs. 8 and 9). At this time, the enzyme formed the closed form shown in Fig. 6. Molecular dynamic simulation was performed according to the method of Kasper *et al.* (Kasper *et al.*, 1996). The simulation could explain the small domain movement of the molecule, but not this side chain movement of Arg292* (data not shown).

Conformational Differences of α-Helix 1 and Its Nearby Loop in the Cn-PLP Complexes

Fig. 10 shows the conformational differences among the Cn-PLP complexes. The hydrophobic substrate analogs were bound near Ile17, Leu18, and Ile37. Ile17 and Leu18 are located at the N-terminal side of α-helix 1, and Ile37 is in the loop region adjacent to α-helix 1. With these interactions, α-helix 1 will move toward the active site on binding of C5-PLP (or C6-PLP). Since Ile17 and Leu18 are in α-helix 1, there was only a slight change of the χ1 angle (the rotation around the C_α-C_β bond) of the side chain (PDB code 1C9C, 1CQ6, 1CQ7, and 1CQ8) (Table III). These residues in the substrate-free holoenzyme and in the C3-PLP and C4-PLP complexes had similar B-factors. These B-factors were higher, suggesting greater flexibility, than those in the C5-PLP and C6-PLP complexes and in the 2-methylaspartate complexes (PDB code 1C9C, 1CQ6, 1CQ7, and 1CQ8) (Table III).

In contrast, Ile37 is situated in the flexible region of the consensus sequence of AspATs (Gly36 – X37 – Gly38, where *X* is isoleucine in *E. coli* AspAT). When C5-PLP or C6-PLP was bound to *E. coli* AspAT, this flexible loop region moved into the active site with a marked change in main chain conformation. The side chain of Ile37 largely moved from the solvent region into the active site (Figs. 9 and 10). The χ1 angles of the

Table III. Properties of the C_α Atoms of Ile17, Leu18, and Ile37

Substrate analog	Enzyme form	χ_1 angle (*degree*)			B-factor ($Å^2$)		
		Ile17	Leu18	Ile37	Ile17	Leu18	Ile37
none (PLP)[a]	open	60.8	-103.5	47.5	71.08	70.66	30.79
C3-PLP	open	-53.5	-53.0	42.6	53.59	53.44	24.81
C4-PLP	open	-61.7	-43.1	28.1	63.76	66.26	45.95
C5-PLP	closed	-67.7	-65.8	190.9	33.53	33.33	18.54
C6-PLP[b]	closed	-66.6	-67.0	-33.4	31.02	32.84	20.47
2MeAsp	closed	-59.2	-69.1	-54.6	31.40	38.14	19.43

[a]AspAT in the substrate-free PLP form (holoenzyme) (PDB code 1ARS) (Okamoto *et al.*, 1994)

[b]AspAT complexed with 2-methylaspartate (PDB code 1ART) (Okamoto *et al.*, 1994)

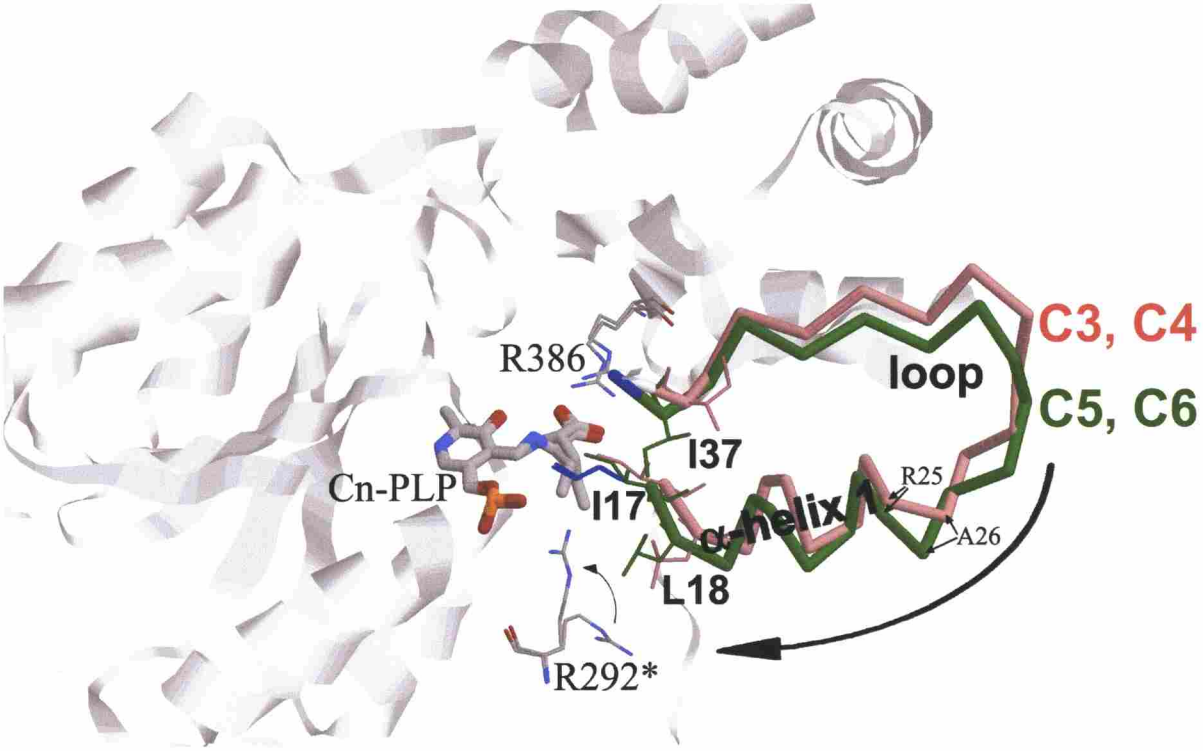

Fig. 10. The mechanisms of domain movement.

The α-helix 1 (Ile17 – Arg25) and the loop region (Ala26 – Ile37) of the C3-PLP or C4-PLP complex in the open form (these residues are colored pink and the others gray) change to the closed form on binding of C5-PLP or C6-PLP (colored green). Ile17 and Ile37 are anchored at the active site by hydrophobic interactions with the substrate. Leu18 is located at the N-terminal end of α-helix 1 and pulls the helix into the active pocket to shield the active site from the solvent. This tugging of residues from Ile17 to Ile37 will change the enzyme from the open to the closed form. This figure was produced using RasMol (CCP4, 1994).

side chain of Ile37 for the C3-PLP, C4-PLP, C5-PLP, and C6-PLP complexes were 43°, 28°, 191°, and −33°, respectively (Table III). These conformational changes are enabled by the presence of glycine on each side of Ile37.

Kinetic Behavior of Mutants of Ile37

Ile37 was replaced by glycine, alanine, valine, and methionine to predict the role of Ile37. The kinetic behaviors of these mutants were summarized in Table IV. The enzymatic activity against hydrophobic amino acid was decreased when Ile37 was replaced by smaller amino acids such as alanine and glycine. The energy required for domain movement (see Discussion) was also increase with this substitution (Table IV).

Comparison between Crystal and Solution Structures

The reactivity of Cys390 against 5,5-dithiobis(2-nitrobenzoic acid) (DTNB) in pig cytoplasmic AspAT is increased during catalysis, when AspAT takes the closed form (Birchmeier *et al.*, 1973; Christen & Metzler, eds., 1985). The Cys390 residue, called "syncatalytic cysteine", is in the small domain, and is far from the catalytic center (~15Å), but situated at the interdomain boundary. In order to confirm that the difference in conformation among the Cn-PLP complexes is not due to differences in

Table IV. Kinetic properties of the half-reactions for mutants of *E. coli* AspAT.[a]

Substrate	$\Delta G_T^{\ddagger}$ (kcal/mol)				
	Ile37Gly	Ile37Ala	Ile37Val	Ile37 (WT)[b]	Ile37Met
C3	18.7	18.1	17.3	17.9	18.2
C4	20.4	18.6	17.5	18.2	19.2
C5	20.0	18.1	17.1	17.6	18.9
C6	19.1	17.4	16.4	16.8	18.0
C7	18.7	17.1	16.1	16.3	17.8
C8	(–)[c]	17.5	16.2	17.0	17.5
$G_{movement}$[d]	4.9	2.0	1.4	1.9	3.1

[a]Conditions: 50 mM HEPES, 100 mM KCl, pH 8.0, and 25 ℃.
[b]Wild type AspAT (Kawaguchi *et al.*, 1997).
[c]Not determined.
[d]The free energy difference between G_{open} and G_{closed}

.

crystal packing, Cys390 was introduced into *E. coli* AspAT and the conformations of the enzyme complexes were monitored in solution by SH titration using DTNB (Fig. 11).

The reaction rates of Cys390 for the C3-PLP and C4-PLP complexes were identical. The rates for the C5-PLP and C6-PLP complexes were also identical and were faster than those for the C3-PLP and C4-PLP complexes. These results coincided with the crystallographic results showing that the C3-PLP and C4-PLP complexes are in the open form and that the C5-PLP and C6-PLP complexes are in the closed form (Figs. 6-10).

Kinetic Background and its Interpretation

The reaction kinetics of AspAT (Fig. 12, open circles) were studied with Cn substrates (Kawaguchi *et al.*, 1997; Kawaguchi & Kuramitsu, 1998). When the free energy difference ($\Delta G_T^{\ddagger}$) between the transition state ($ES^{\ddagger}$) and the unbound enzyme plus the substrate (E + S) (Fig. 5) was plotted against the total number of carbon atoms in the substrate, a linear correlation was observed for substrates from C5 to C7 (Fig. 12). This linear relationship suggests a uniform hydrophobic environment of the substrate-binding site. A similar uniform environment has been suggested for horseradish peroxidase (Ryu & Dordick, 1992), *Bacillus amyloliquefaciens* subtilisin (Wangikar *et al.*, 1995), *Paracoccus*

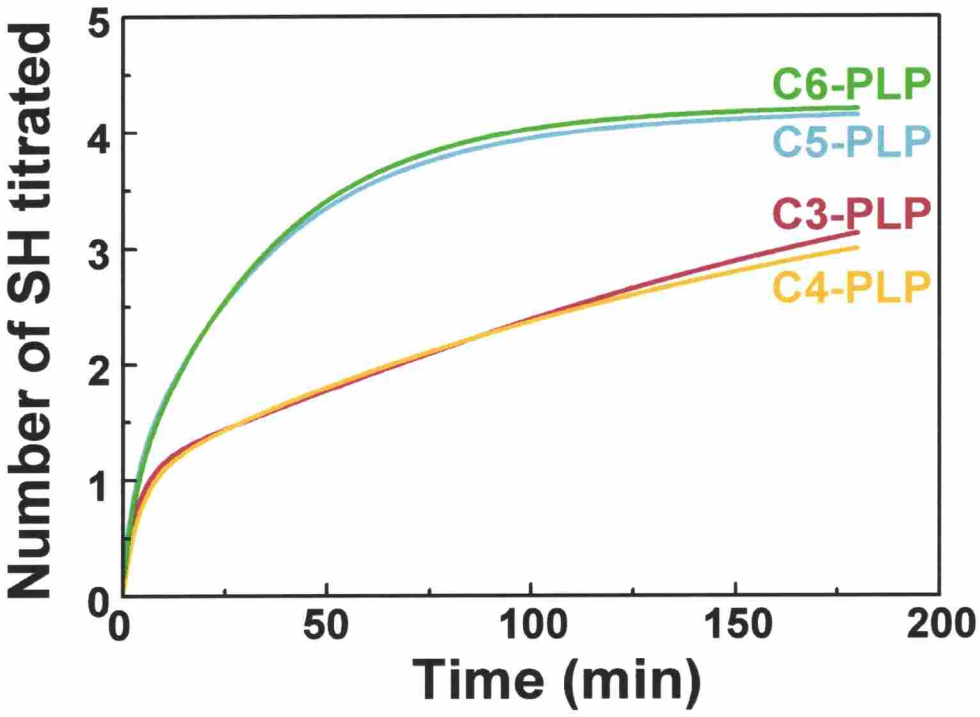

Fig. 11. Time dependence of the titration of SH groups with DTNB. The titration curves for the C3-PLP and C4-PLP complexes, with the open form, are distinct from the curves for the C5-PLP and C6-PLP complexes, with the closed form (Figs. 6-10). The reaction of SH groups of the enzyme with DTNB was monitored spectrophotometrically at 412 nm, pH 8.0, 25 °C.

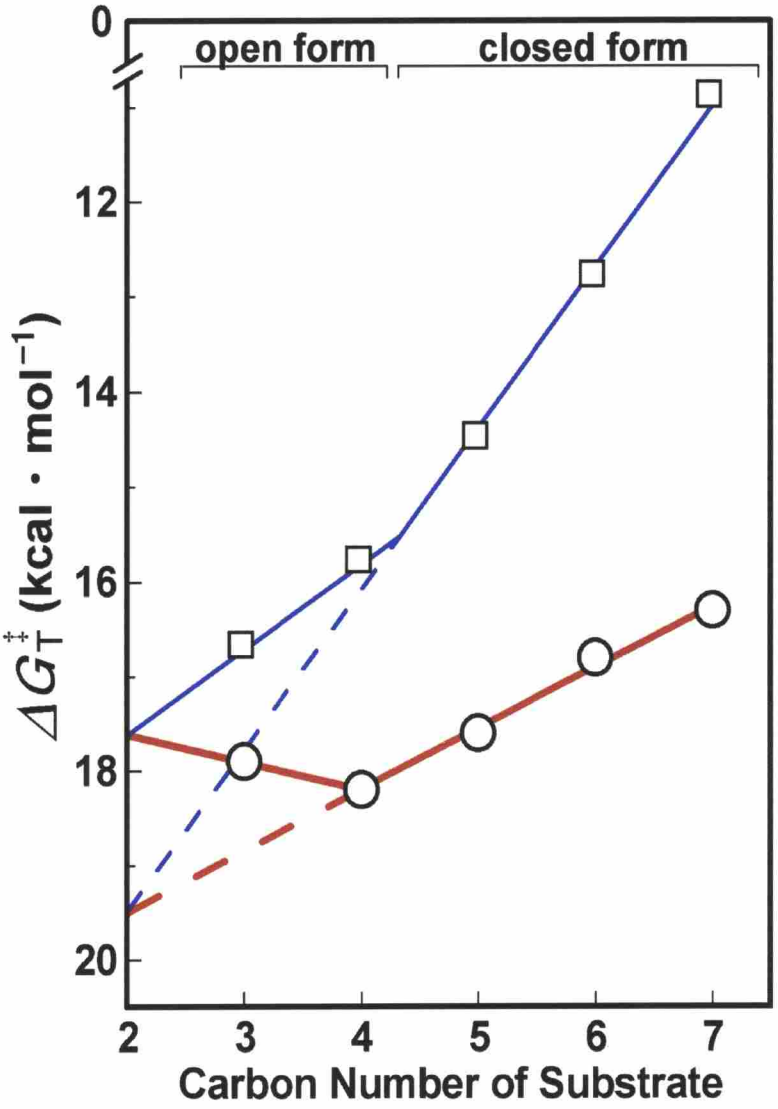

Fig. 12. Correlation between $\Delta G_T^{\ddagger}$ and the number of carbon atoms in the substrate for aspartate aminotransferase (O) and aromatic amino acid aminotransferase (□).

The substrates (Cn substrates) are a series of aliphatic amino acids with linear side chains: $CH_3(CH_2)_{n-3}C_{(\alpha)}H(NH_3^+)COO^-$ (Fig. 3). The free energy difference ($\Delta G_T^{\ddagger}$) between the unbound enzyme plus substrate (E + S) and the transition state ($ES^{\ddagger}$) (see Fig. 5) was calculated using the equation $\Delta G_T^{\ddagger} = RT(\ln(k_BT/h) - \ln(k_{max}/K_d))$ (Eq. 5). The buffer solution contained 50 mM HEPES and 100 mM KCl, pH 8.0, at 25 °C.

For each enzyme, solid line fitted to the data for C5, C6, and C7 was extrapolated to C2 (dotted line). This line represents the $\Delta G_T^{\ddagger}$ value for the closed form of the enzyme. The solid line fitted to the data for C3 and C4 represents the $\Delta G_T^{\ddagger}$ value for the open form of the enzyme (see the text for details).

denitrificans AroAT (Oue *et al.*, 1997), and bovine α–chymotrypsin (Dorovska *et al.*, 1972) (see Fig. 13). In all the above cases, the substrate-binding pockets consist of different kinds of atoms. The linear kinetic relationship of these enzymes will be accomplished by fluctuation of the active site. Although the detailed reasons for this linear relationship remain to be elucidated, it was found to be useful for estimating the energy required for domain movement, as described in Discussion.

For AspAT, the maximum value of 18.2 kcal mol^{-1} was observed with C4 (Fig. 12). The change of slope around C4 reflects the hydrophobicity of the active site. This conversion of the active site environment could be explained by the domain movement of the enzyme molecule, which is accompanied by expulsion of bulk water molecules from the active site (see below).

a

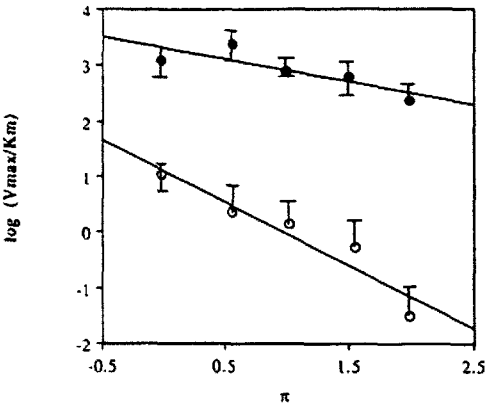

FIGURE 1: Effect of substrate hydrophobicity (π) on the catalytic efficiency of HRP in (●) aqueous buffer and (○) butyl acetate containing 1% aqueous buffer. A summary of the δ values is given in Table II. Phenol concentrations ranged from 0.5 mM to 1 M, and saturation kinetics were observed in aqueous buffer and aqueous dioxane solutions (see Figure 2). Peroxidase concentration was varied from 0.1–1 μg/mL in aqueous buffer to 1–10 μg/mL in organic media. The concentration of H_2O_2 was 0.25 mM in all experiments. Values of π for phenolic substrates are given in Table I. Error bars (in this and relevant subsequent figures) indicate the standard deviation of the kinetic measurements, performed in triplicate.

b

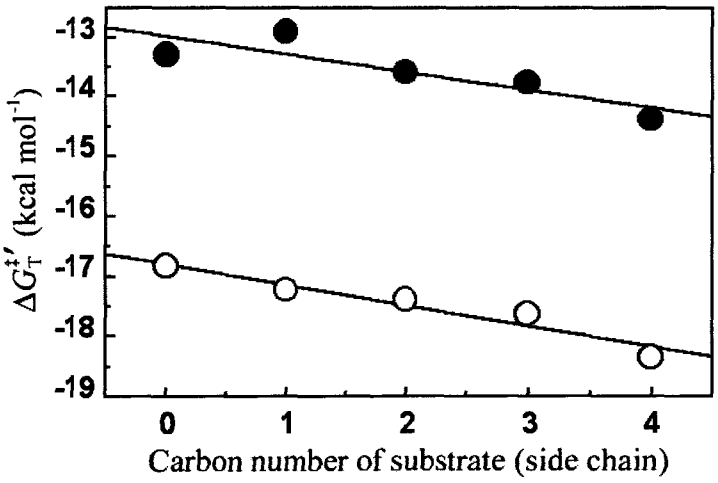

Fig. 13-1. Correlation between $\Delta G_T^{\ddagger}$ and the carbon number of substrate for horseradish peroxidase.

a, the original data (horseradish peroxidase (Ryu & Dordick, 1992)). b, replotting the original data against the carbon number of substrate.

a

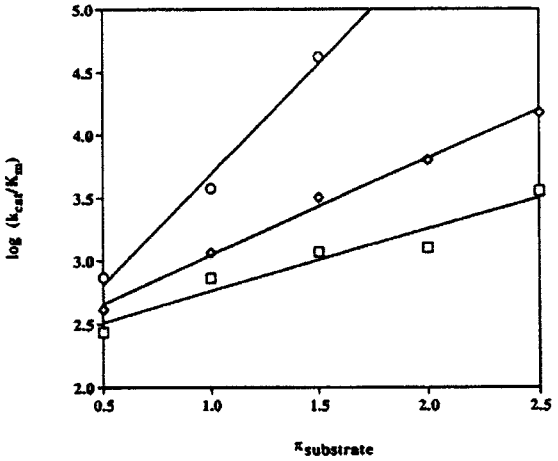

FIGURE 1: Effect of substrate hydrophobicity on the catalytic efficiency of subtilisin BPN' and two hydrophobic mutants: (□) wild type; (◇) G166A; (○) G166V. Catalytic efficiencies were measured as described in the Experimental Procedures. The G166V mutant shows considerable steric hindrance for large hydrophobic substrates and, thus, was limited to *N*-Ac-L-Ala, *N*-Ac-L-aminobutyric acid, and *N*-Ac-L-norvaline as substrates. Values of k_{cat}/K_m are in $M^{-1}\ s^{-1}$.

b

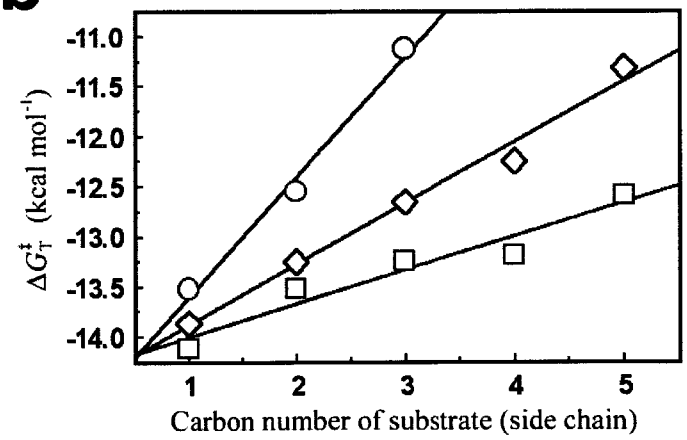

Fig. 13-2. Correlation between $\Delta G_T^{\ddagger}$ and the carbon number of substrate for *Bacillus amyloliquefaciens* subtilisin.

a, the original data (*Bacillus amyloliquefaciens* subtilisin (Wangikar *et al.*, 1995)). b, replotting the original data against the carbon number of substrate.

a

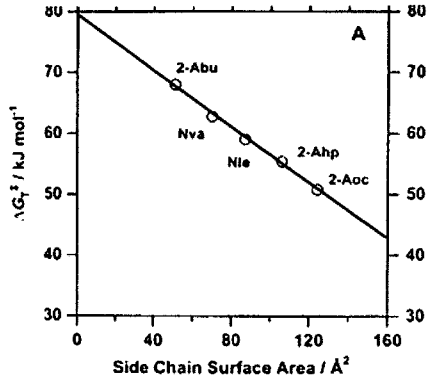

Fig. 5. Activation free energy ($\Delta G_T^{\ddagger}$) values for the reaction of pdArAT (A), ecArAT (B), or ecAspAT (C) with neutral amino acids plotted against the surface area of the amino acid side chains. pH 8.0, 25 C. The letters beside the plots denote amino acids: 2-Abu, 2-amino-butyrate; Nva, norvaline; Leu, leucine; Nle, norleucine; 2-Ahp, 2- aminoheptanoate; 2-Aoc, 2-aminooctanoate; Phe, phenylalanine; Tyr, tyrosine; Trp, tryptophan. Straight-chain aliphatic amino acids are shown by open circles, and other amino acids byclosed circles. The free energy difference ($\Delta G_T^{\ddagger}$) between the transition state for the half transamination reaction ($ES^{\ddagger}$) and unbound enzyme plus substrate (E + S) was calculated from the k_{cat}^{app}/K_m^{app} values listed in Tables I and III using the equation $\Delta G_T^{\ddagger} = RT[\ln(k_b T/h) - \ln(k_{cat}^{app}/K_m^{app})]$ (37). Side chain surface area for each amino acid was calculated using Quanta (version 4.0, Molecular Simulations, Waltham, MA) for the CHARMm-minimized conformation.

b

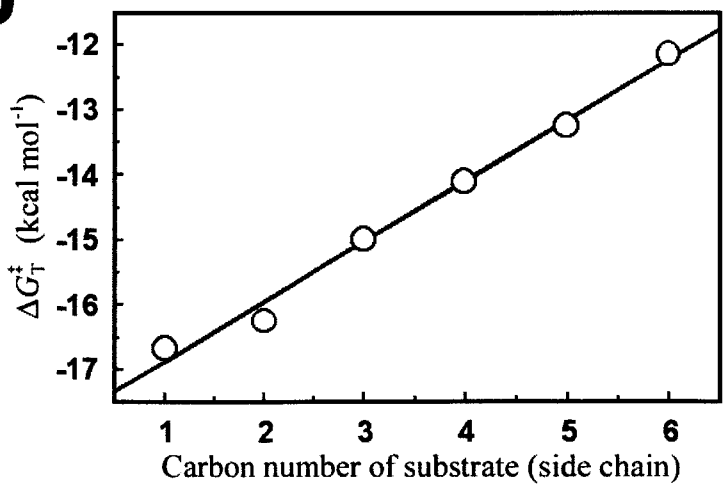

Fig. 13-3. Correlation between $\Delta G_T^{\ddagger}$ and the carbon number of substrate for *Paracoccus denitrificans* AroAT.

a, the original data (*Paracoccus denitrificans* AroAT (Oue *et al.*, 1997)). b, replotting the original data against the carbon number of substrate.

a

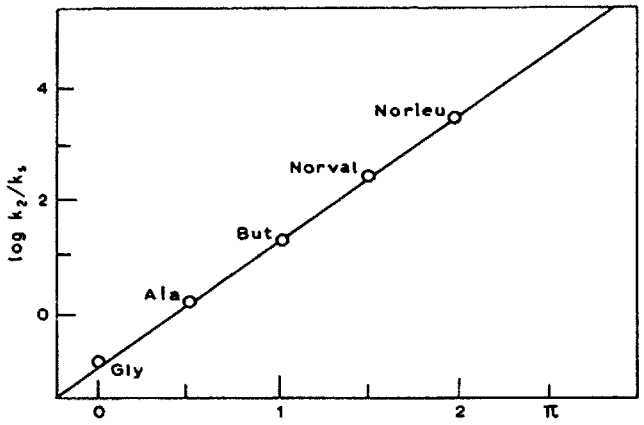

Fig. 2. The values of rate constants (k_2/K_s) for chymotryptic hydrolysis of methyl esters of *N*-acetyl-L-amino acids, $RCH(NHCOCH_3)C(O)OCH_3$, against the hydrophobicity π of corresponding R substituents. Experimental conditions are given in the table. The π values are the Hansch constants for the R substituents [2].

b

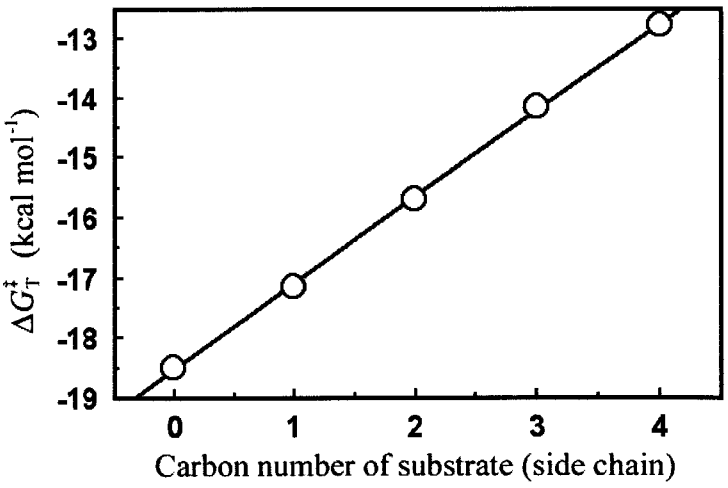

Fig. 13-4. Correlation between $\Delta G_T^{\ddagger}$ and the carbon number of substrate for bovine α-chymotrypsin.

a, the original data (bovine α-chymotrypsin (Dorovska et al., 1972)). b, replotting the original data against the carbon number of substrate.

Discussion

Mechanism of Domain Movement

Many enzymes undergo a large conformational change that serves to expel bulk solvent from the active site and to properly position functional groups for catalysis. This movement, in response to substrate binding at the active site, was termed "induced fit" by Koshland, and implies that multiconformational states of enzymes are in equilibrium with one another and are easily perturbed by ligands (Koshland, 1958). Many experiments with a number of proteins have revealed domain movement in aqueous solution by using substrate analogs, or have directly revealed movement by X-ray crystallography; examples are myosin (Maruta *et al.*, 1999), glutathione S-transferase (Neuefeind *et al.*, 1997), tryptophan synthase (Rhee *et al.*, 1998), and maltodextrin phosphorylase (O'Reilly *et al.*, 1997).

AspATs from *E. coli* and many vertebrates have a flexible loop (in the case of E. coli AspAT, Gly36 – Ile37 – Gly38) and an α-helix 1 near the N-terminus of the protein (6-9; Figs. 6, 9, and 10). The residues Ile37 in the flexible loop and Ile17 and Ile18 in α-helix 1 are very important for domain movement.

In the case of catalysis of a series of aliphatic substrates (Figs. 6, 9, and 10), Ile37 in the flexible loop and Ile17 and Leu18 in α-helix 1 interact

with longer substrates (Cn, n ≥ 5) and recognize the substrate as a hydrophobic plate. The interaction of these residues with the bound substrate will pull α-helix 1 to cover the active-site entrance, and will trigger domain movement.

This is also the case for acidic substrates (aspartate, glutamate, or their keto acids). The negatively charged carboxyl group of the substrate is neutralized by the positively charged Arg292*. These neutralized groups will also be recognized as a hydrophobic plate by Ile37, Ile17, and Ile18, as described above.

To confirm the validity of this hypothesis, the isoleucine residue at the position of 37 was substituted with various hydrophobic amino acids (glycine, alanine, valine, and methionine). This substitution caused decrease in the reactivity against aliphatic amino acid. I tried to estimate the energy required for domain movement (see *Estimation of Energy Required for Domain Movement* in Discussion) for these mutants. I could observe the decrease in the energy when Ile37 was replaced by smaller amino acid residues (Table IV). This observation indicates that the 37th residue might act as sensor for domain closure. When, the I37G mutation was introduced into *E. coli* AspAT, this mutant could not undergo any domain movement on substrate binding with either acidic or hydrophobic C6 substrate (Figs 14 and 15).

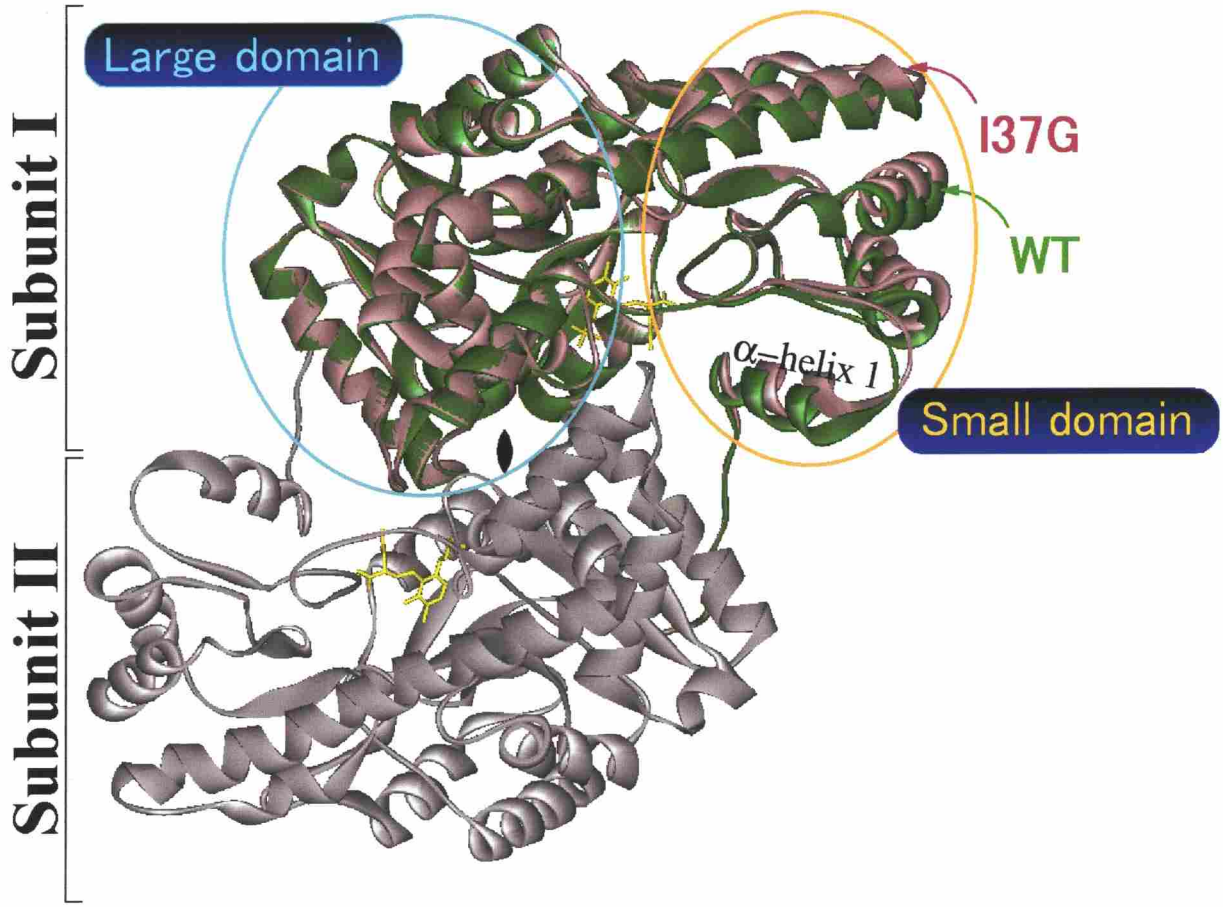

Fig. 14. Overall structure of wild-type AspAT and Ile37Gly mutant complexed with acidic substrate analogs.

Ile37Gly mutant of AspAT complexed with Asp-PLP (this work) (pink) was superimposed onto wild-type AspAT complexed with 2-methylaspartate (PDB code 1ART (Okamoto *et al,* 1994)) (green). AspAT undergoes a large domain movement when it binds to acidic substrates. The movement of α–helix 1 toward active site are observed for the both cases. This figure was produced using WebLab ViewerLite (MSI).

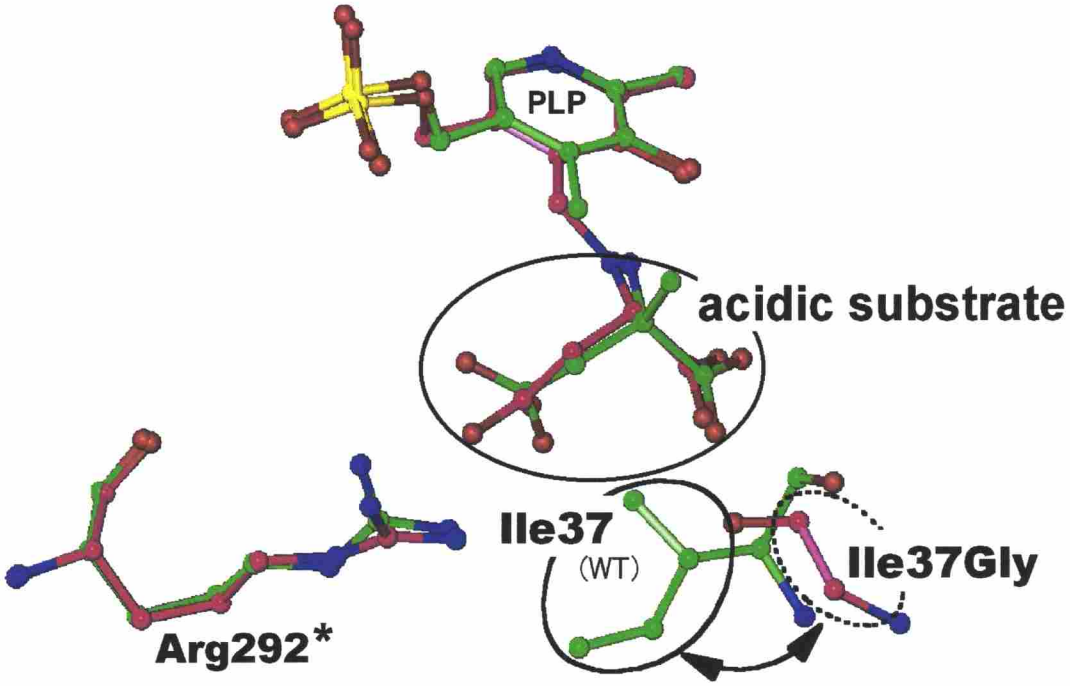

Fig. 15. Ile37 and Arg292 of AspAT and its mutant enzyme bound with acidic substrate analogs.

The structure of the Ile37Gly mutant of AspAT complexed with Asp-PLP (magenta) (this work) and wild-type AspAT complexed with 2-methylaspartate (PDB code 1ART(Okamoto *et al,* 1994)) (green). The atomic position of C_α atom in the 37th residue was drastically changed between the wild-type enzyme and Ile37Gly mutant. These figures were produced using program O (Jones *et al.*, 1991).

Estimation of Energy Required for Domain Movement

Previous crystallographic studies have indicated that AspAT takes either an open or a closed form, but never takes an intermediate state (Christen & Metzler, eds., 1985; Smith *et al.*, 1989; Kamitori *et al.*, 1990; Jäger *et al.*, 1994; Miyahara *et al.*, 1994; Okamoto *et al.*, 1994). On binding of an acidic substrate, the enzyme molecule undergoes a large domain movement. Arg292* moves from the outside to the inside of the active site, and recognizes the ω-carboxyl group of the substrate (Christen & Metzler, eds., 1985; Smith *et al.*, 1989; Kamitori *et al.*, 1990; Jäger *et al.*, 1994; Miyahara *et al.*, 1994; Okamoto *et al.*, 1994).

For hydrophobic substrates, Arg292* was expected to remain outside the active site (Malashkevich *et al.*, 1995; Kawaguchi *et al.*, 1997; Malashkevich *et al.*, 1999). In this study, however, movement of the side chain of Arg292* and domain closure (Figs. 6-10) were observed for longer hydrophobic substrate analogs ($C \geq 5$).

From the following reasonable assumptions, the free energy required for domain movement was estimated (Figs. 16 and 17). These assumptions were supported by comparison with the homologous enzyme *E. coli* aromatic amino acid aminotransferase (AroAT), as discussed in the "*Confirmation from a Homologous Enzyme*" section of Discussion.

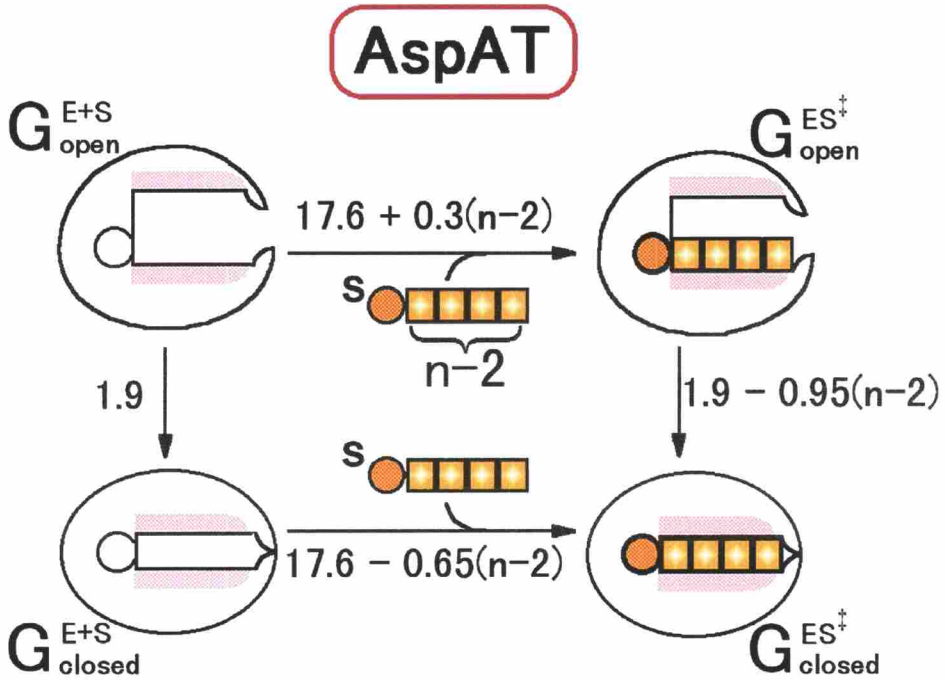

Fig. 16. Thermodynamic cycle of AspAT.

Summary of thermodynamic cycles (Fig. 17) for the reactions of AspAT with a series of substrates from C3 to C7. The number n represents the number of carbon atoms in the substrate. $G_{\text{open}}^{\text{E+S}}$ represents the sum of the free energy of an enzyme with unbound open form ($G_{\text{open}}^{\text{E}}$) and that of a substrate (G^{S}). $G_{\text{closed}}^{\text{E+S}}$ represents the sum of the free energy of an enzyme with unbound closed form ($G_{\text{closed}}^{\text{E}}$) and that of a substrate (G^{S}). $G_{\text{open}}^{\text{ES}\ddagger}$ and $G_{\text{closed}}^{\text{ES}\ddagger}$ are the transition states of the open and closed forms, respectively, of the complex (see text for details).

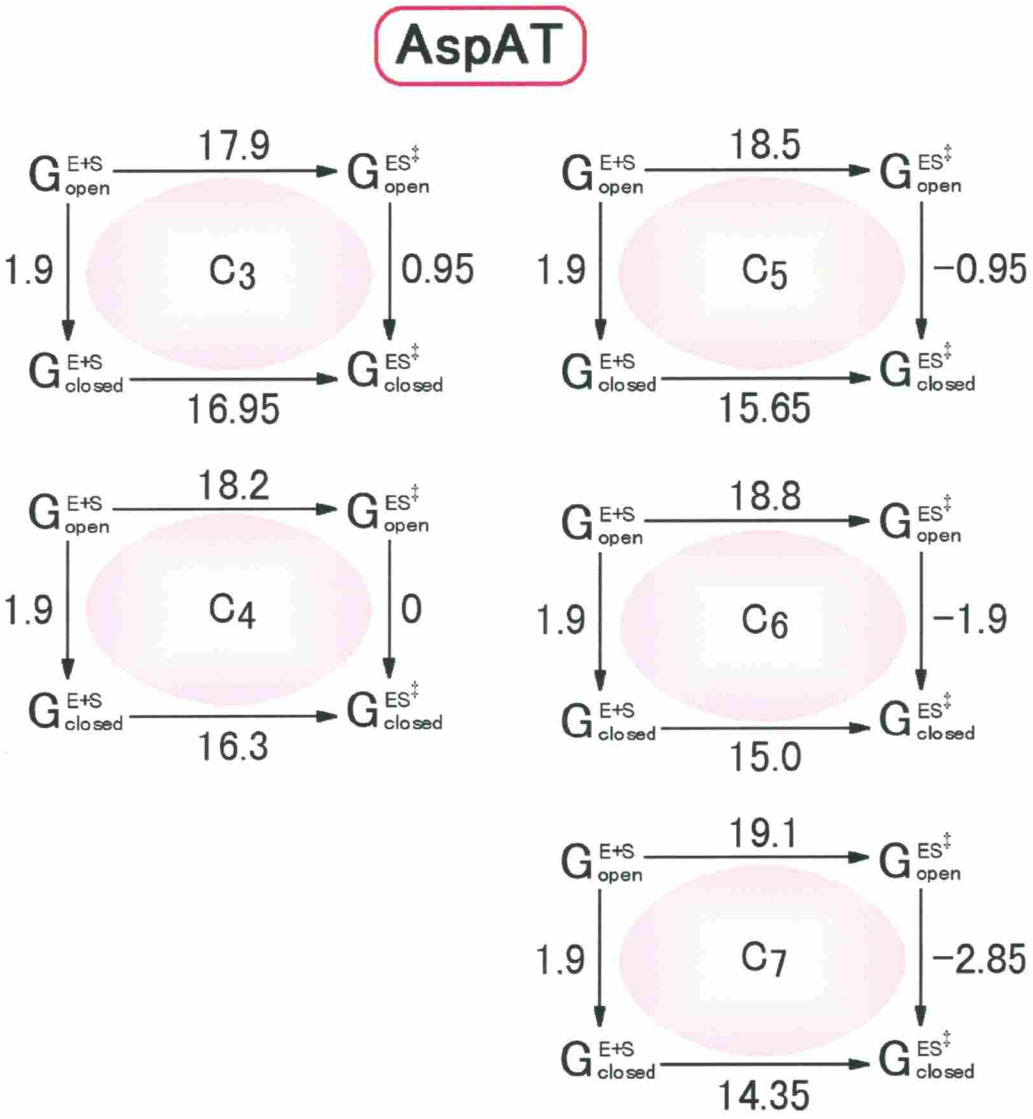

Fig. 17. Thermodynamic cycle of Fig. 16 for each substrate.

The thermodynamic cycle for each substrate was calculated from the data points in Fig. 12. From these data, the energy required for domain closure of AspAT was estimated to be 1.9 kcal mol^{-1} (see text for details).

Assumption 1: The energy contribution of each constituent group of the substrate CH_3-, -CH_2-, and -$C_{(\alpha)}H$ (NH_3^+) COO^- groups was additive.

Assumption 2: The energy contribution of the group -$C_{(\alpha)}H(NH_3^+)COO^-$ was identical for all the substrates studied.

This assumption is based on the following results:

(*a*) the crystallographic analyses (Figs. 6-10); and

(*b*) the linearity of $\Delta G_T^{\ddagger}$ vs. the total number of carbon atoms in the substrate (Fig. 12).

Assumption 3: The hydrophobic environment around the substrate-binding pocket is uniform, and the energy contribution of the methylene and methyl groups is identical.

This assumption is supported by the linearity of $\Delta G_T^{\ddagger}$ from C5 to C7 substrates in Fig. 12.

From these assumptions, I tried to make thermodynamic cycles of AspAT for Cn substrates, and I estimated the free energy differences among molecular species. G_{open}^{E+S} and G_{closed}^{E+S} in Fig. 16 represent the Gibb's free energy for the open and closed forms, respectively, where G_{open}^{E+S} or G_{closed}^{E+S} is the sum of free energies of the unbound enzyme (G^E) and unbound

substrate (G^S). $G_{open}^{ES‡}$ and $G_{closed}^{ES‡}$ represent the open and closed forms, respectively, complexed with Cn substrate in the transition state. Whether the enzyme will be closed depends on the energy difference between $G_{open}^{ES‡}$ and $G_{closed}^{ES‡}$.

From the crystallographic results in Fig. 6, I found that the conformations of the C5-PLP and C6-PLP complexes were in the closed form and that the conformations of the C3-PLP and C4-PLP complexes were in the open form. Therefore the slope from C5 to C7 (–0.65 kcal mol^{-1}) in Fig. 12 represents the energy obtained from the hydrophobic interaction between the substrate and the substrate-binding pocket of the closed form enzyme. On the other hand, the slope from C3 to C4 (+0.3 kcal mol^{-1} CH_2^{-1}) represents the energy loss due to contact between the hydrophobic substrate and the hydrophilic surface of the active pocket filled with water molecules. In Fig. 12, the extrapolated red line for AspAT (dotted line) coincides at C = 2 with $\Delta G_T^‡$ = 19.5 kcal mol^{-1}. This $\Delta G_T^‡$ corresponds to the energy difference between G_{open}^{E+S} and $G_{closed}^{ES‡}$ in Fig. 16. The slope of this extrapolated line (–0.65 kcal mol^{-1} CH_2^{-1} for AspAT) corresponds to the hydrophobicity of the substrate-binding pocket for the closed form of AspAT.

The C3-PLP or C4-PLP complex is in the open form (Figs. 6, 7, and 10). If the $\Delta G_T^‡$ values for the open form was extrapolated to C2, the

$\Delta G_T^{\ddagger}$ value of 17.6 kcal mol^{-1} was obtained (Fig. 12, red solid line). This $\Delta G_T^{\ddagger}$ corresponds to the energy difference between G_{open}^{E+S} and $G_{open}^{ES^{\ddagger}}$ in Fig. 16.

As described above, the $\Delta G_T^{\ddagger}$ value for the closed form (from C5 to C7) corresponds to $G_{closed}^{ES^{\ddagger}}$ - G_{open}^{E+S} and that for the open form (from C3 to C4) corresponds to $G_{open}^{ES^{\ddagger}}$ - G_{open}^{E+S}. Both the X-ray crystallographic and kinetic results showed that the conformation around $-C_{(\alpha)}H(NH_3^+)COO^-$ was identical between the open form, which corresponds to $G_{open}^{ES^{\ddagger}}$, and the closed form, which corresponds to $G_{closed}^{ES^{\ddagger}}$. Based on these results, It was suggested that the energy changes from the open (G_{open}) to closed (G_{closed}) forms are similar between bound ($G^{ES^{\ddagger}}$) and unbound (G^{E+S}) enzymes. Since the free energy of unbound substrate (G^S) is included in both G_{closed}^{E+S} and G_{open}^{E+S} in Fig. 16, this energy difference corresponds to the energy for conformational change of an unbound enzyme from the open (G_{open}^{E}) to closed (G_{closed}^{E}) forms. The free energy change thus estimated for domain movement ($G_{closed}^{E} - G_{open}^{E}$) is 1.9 kcal mol^{-1} for aspartate aminotransferase.

Confirmation from a Homologous Enzyme

E. coli aromatic amino acid aminotransferase [EC 2.6.1.57] (AroAT) is an isozyme of AspAT and catalyzes transamination reactions with substrate specificity different from that of AspAT (Kuramitsu *et al.*, 1985a;

Kuramitsu *et al.*, 1985b; Hayashi *et al.*, 1993; Ko *et al.*, 1999). When I applied my analysis to the kinetic data of AroAT (Fig. 18), I could confirm the correctness of my analysis, and I obtained the same energy of 1.9 kcal mol^{-1} for domain closure as that found for AspAT as follows.

The amino acid sequence of AroAT is 43% identical to that of AspAT, and both enzymes consist of two identical subunits of 44 kDa (Kuramitsu *et al.*, 1985a; Kuramitsu *et al.*, 1985b). The pK_a values of the PLP – Lys258 Schiff base are also very similar between AspAT and AroAT (Hayashi *et al.*, 1993), suggesting the similarity of the microenvironment of their active pockets. The similarity of the conformations of these enzymes was confirmed by X-ray crystallography (Okamoto *et al.*, 1994; Ko *et al.*, 1999). The root-mean-square deviation between the unliganded form of AspAT (PDB code 1ASN) and AroAT (PDB code 3TAT) is 1.28 Å for the overall structure (Ko *et al.*, 1999). When I applied the least-squares fit to the C_α atoms of the large domain residues of the unliganded forms of AspAT (PDB code 1ARS) and AroAT (PDB code 3TAT), the deviation was 1.85 Å for the overall structure. I also applied the least-squares fit to the 25 C_α atoms in the active pocket (the residue numbers are 36, 37, 70*, 107, 108, 109, 110, 140, 141, 142, 143, 189, 194, 222, 224, 225, 256, 257, 258, 263, 266, 292*, 296*, 297*, and 386, where * represents a residue from another subunit). The root-mean-square

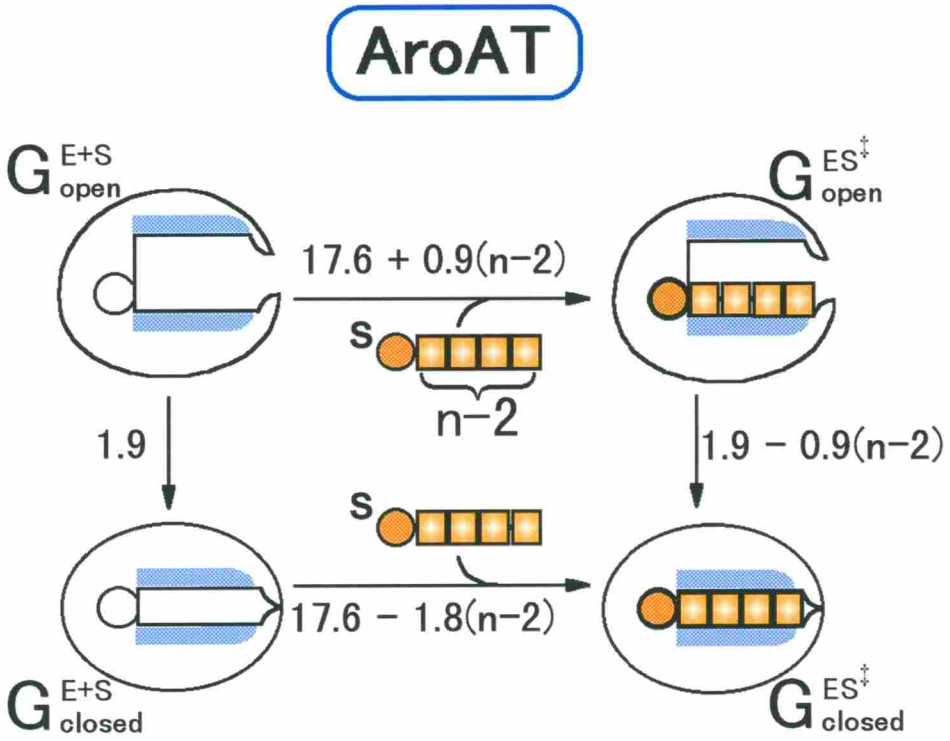

Fig. 18. Thermodynamic cycle of AroAT.

Summary of thermodynamic cycles for AroAT. This figure was obtained by the similar method as described for AspAT (see Figs. 12, 16, and 17).

deviation of these residues was 0.76 Å. The active site residues around the group $-C_{(\alpha)}H(NH_3^+)COO^-$ of the substrate (Ile37, Asn194, Tyr225, Tyr258, Met359, Phe360, and Arg386) are completely conserved (Kuramitsu *et al.*, 1985a; Kuramitsu *et al.*, 1985b) and the root-mean-square deviation was 0.56 Å for the C_α atoms. These findings suggest that these two enzymes have similar catalytic mechanisms with similar three-dimensional structures.

On the basis of these structural similarities between AspAT and AroAT, I applied the same kinetic analysis to AroAT (Figs. 12 and 18). The extrapolated blue dotted line for AroAT in Fig. 12 coincided with the extrapolated red line for AspAT at C = 2 with $\Delta G_T^{\ddagger} = 19.5$ kcal mol^{-1}. The coincidence between the two enzymes suggests that the energy contribution of the $-C_{(\alpha)}H(NH_3^+)COO^-$ group in the "closed form" of the enzyme is 19.5 kcal mol^{-1} and that the environment around the binding site of $-C_{(\alpha)}H(NH_3^+)COO^-$ is identical in AspAT and AroAT. The slope of this extrapolated line, which corresponds to the hydrophobicity of the substrate-binding pocket for the closed form, was –1.7 kcal mol^{-1} CH_2^{-1} for AroAT. This value was smaller than that of –0.65 kcal mol^{-1} CH_2^{-1} for AspAT.

On the other hand, if I extrapolate the $\Delta G_T^{\ddagger}$ values for AroAT between C3 and C4 to C2, I obtain a value for $\Delta G_T^{\ddagger}$ of 17.6 kcal mol^{-1} (Fig. 12, solid blue line). This line for AroAT coincides with the line for AspAT at C2.

This coincidence between the two "open form" aminotransferases suggests that the environment around the binding site of $-C_{(\alpha)}H(NH_3^+)COO^-$ is identical in AspAT and AroAT. In summary, these observations indicate that the active pocket environment for the open and closed forms is almost identical in AspAT and AroAT except for the hydrophobicity of the substrate-binding pocket.

The free energy required for domain movement of AroAT (Fig. 18), obtained by the same method used for AspAT, was estimated to be 1.9 kcal mol^{-1}. The identity of the energy for domain movement in these two aminotransferases supports the correctness of my analysis.

Comparison with Other Results Related to Domain Movement

A number of previous studies have also attempted to analyze domain movement. Pfister *et al.* (Pfister *et al.*, 1985) measured the hydrogen-deuterium exchange of pig cytosolic AspAT and estimated the energy difference between open and closed forms to be 2-3 kcal mol^{-1}. Since the hydrogen-deuterium exchange reflects not only domain movement but also the fluctuation of the domain itself, it is difficult to isolate the contribution of the domain movement from the data. Rhee *et al.* (Rhee *et al.*, 1997) estimated the free energy for burying the hydrophobic plug (Pro14 –

Phe18) of pig cytosolic aspartate aminotransferase into the active site to be 5.3 kcal mol^{-1} and concluded that the energy is more than enough to drive the conformational change. Radmacher *et al.* (Radmacher *et al.*, 1994) measured height fluctuations on top of the lysozyme molecule with an atomic force microscope and suggested that the energy for this fluctuation is about 3 kcal mol^{-1}, although they recommended caution when interpreting whether or not the height changes correspond directly to a change in the diameter of the enzyme. Karplus and McCammon (Karplus & McCammon, 1983) used molecular dynamic simulation to predict domain movement, but they did not quantitatively estimate the energy required for the process. The data obtained from single-molecule measurements of myosin movement along an actin filament (Mehta *et al.*, 1999) might also correspond to the energy of domain movement.

Conclusion

In this study, I tried to estimate the energy required for domain movement from thermodynamic analysis. The estimated energy of 2 kcal mol^{-1} is only three times as large as the energy of thermal fluctuations. This energy for domain closure of about 2 kcal mol^{-1} predicts that the enzyme fluctuates between the open and closed forms with a molar ratio of about 30:1 ($RT \ln(30/1) = 2$ kcal mol^{-1}). By using this domain fluctuation,

an enzyme searches for its substrate; tight binding to the substrate then follows.

References

Ames, J. B., Ishima, R., Tanaka, T., Gordon, J. I., Stryer, L., and Ikura, M. (1997) Molecular mechanics of calcium-myristoyl switches. *Nature* **389,** 198-202

Bennett, M. J., Choe, S., and Eisenberg, D. (1994) Domain swapping: entangling alliances between proteins. *Proc. Natl. Acad. Sci. U. S. A.* **91,** 3127-3131

Bernstein, B. E., Michels, P. A., Hol, W. G. (1997) Synergistic effects of substrate-induced conformational changes in phosphoglycerate kinase activation. *Nature* **385,** 275-278

Birchmeier, W., Wilson, K. J., and Christen, P. (1973) Cytoplasmic aspartate aminotransferase: syncatalytic sulfhydryl group modification. *J. Biol. Chem.* **248,** 1751-1759

Birktoft, J. J., Rhodes, G., and Banaszak, L. J. (1989) Refined crystal structure of cytoplasmic malate dehydrogenase at 2.5-Å resolution. *Biochemistry* **28,** 6065-6081

Brünger, A. T. (1993) X-PLOR version 3.1 a system for X-ray crystallography and NMR (Yale Univ. Press, New Haven)

Cheng, X., Kumar, S., Posfai, J., Pflugrath, J. W., and Roberts, R. J. (1993) Crystal structure of the *Hha*I DNA methyltransferase complexed with S-adenosyl-L-methionine. *Cell* **74,** 299-307

Christen, P. and Metzler, D. E., eds. (1985) Transaminase, Wiley and Sons, New York

Collaborative Computational Project, Number 4. (1994) The CCP4 Suite: Programs for Protein Crystallography *Acta Crystallogr.* D**50**, 760-763

Concha, N. O., Head, J. F., Kaetzel, M. A., Dedman, J. R., and Seaton, B. A. (1993) Rat annexin V crystal structure: Ca^{2+}-induced conformational changes. *Science* **261,** 1321-1324

Derewenda, U., Brzozowski, A. M., Lawson, D. M., and Derewenda, Z. S. (1992) Catalysis at the interface: the anatomy of a conformational change in a triglyceride lipase. *Biochemistry* **31,** 1532-1541

Dorovska, V. N., Varfolomeyev, S. D., Kazanskaya, N. F., Klyosov, A. A., and Martinek, K. (1972) The influence of the geometric properties of the active centre on the specificity of α-chymotrypsin catalysis. *FEBS Lett.* **23,** 122-124

Fersht, A. (1985) Enzyme-substrate complementarity, and binding energy in catalysis. In Enzyme structure and mechanism (Fersht, A., ed.), 2nd edit., pp311-346. W. H. Freeman and Company, New York.

Fitzgerald, P. M., McKeever, B. M., VanMiddlesworth, J. F., Springer, J. P., Heimbach, J. C., Leu, C. T., Herber, W. K., Dixon, R. A., and Darke, P.L. (1990) Crystallographic analysis of a complex between human immunodeficiency virus type 1 protease and acetyl-pepstatin at 2.0-Å resolution. *J. Biol. Chem.* **265,** 14209-14219

Gerstein, M. and Chothia, C. (1991) Analysis of protein loop closure. Two types of hinges produce one motion in lactate dehydrogenase. *J. Mol. Biol.* **220,** 133-149

Gerstein, M., and Krebs, W. (1998) A database of macromolecular motions. *Nucleic Acids Res.* **26,** 4280-4290

Hayashi, H., Inoue, K., Nagata, T., Kuramitsu, S., and Kagamiyama, H. (1993) *Escherichia coli* aromatic amino acid aminotransferase: Characterization and comparison with aspartate aminotransferase. *Biochemistry* **32**, 12229-12239

Jäger, J., Moser, M., Sauder, U., and Jansonius, J. N. (1994) Crystal structures of *Escherichia coli* aspartate aminotransferase in two conformations. Comparison of an unliganded open and two liganded closed forms. *J. Mol. Biol.* **239**, 285-305

Jones, T. A., Zou, J. Y., Cowan, S. W., and Kjeldgaard, M. (1991) Improved methods for binding protein models in electron density maps and the location of errors in these models. *Acta Crystallogr.* **A47**, 110-119

Kamitori, S., Hirotsu, K., Higuchi, T., Kondo, K., Inoue, K., Kuramitsu, S., Kagamiyama, H., Higuchi, Y., Yasuoka, N., Kusunoki, M., and Matsuura, Y. (1987) Overproduction and preliminary X-ray characterization of aspartate aminotransferase from *Escherichia coli*. *J. Biochem. (Tokyo)* **101,** 813-816

Kamitori, S., Okamoto, A., Hirotsu, K., Higuchi, T., Kuramitsu, S., Kagamiyama, H., Matsuura, Y., and Katsube, Y. (1990) Three-dimensional structures of aspartate aminotransferase from *Escherichia coli* and its mutant enzyme at 2.5 Å resolution. *J. Biochem (Tokyo)* **108**, 175-184

Karplus, M. and McCammon, J. A. (1983) Dynamics of proteins: Elements and function. *Annu. Rev. Biochem.* **52**, 263-300

Kasper, P., Sterk, M., Christen, P., and Gehring, H. (1996) Molecular-dynamics simulation of domain movements in aspartate aminotransferase. *Eur. J. Biochem.* **240,** 751-755

Kawaguchi, S. and Kuramitsu, S. (1998) Thermodynamics and molecular simulation analysis of hydrophobic substrate recognition by aminotransferases. *J. Biol. Chem.* **273**, 18353-18364

Kawaguchi, S., Nobe, Y., Yasuoka, J., Wakamiya, T., Kusumoto, S., and Kuramitsu, S. (1997) Enzyme flexibility: a new concept in recognition of hydrophobic substrates. *J. Biochem. (Tokyo)* **122**, 55-63

Kiick, D. M. and Cook, P. F. (1983) pH studies toward the elucidation of the auxiliary catalyst for pig heart aspartate aminotransferase. *Biochemistry* **22**, 375-82

Ko, T. P., Wu, S. P., Yang, W. Z., Tsai, H., and Yuan, H. S. (1999) Crystallization and preliminary crystallographic analysis of the *Escherichia coli* tyrosine aminotransferase. *Acta Crystallogr.* **D55**, 1474-1477

Koshland, D. E., Jr. (1958) Application of a theory of enzyme specificity to protein synthesis. *Proc. Natl. Acad. Sci. U. S. A.* **44**, 98-104

Kuramitsu, S., Hamaguchi, K., Ogawa, T., and Ogawa, H. (1981) A large-scale preparation and some physicochemical properties of RecA protein. *J. Biochem. (Tokyo)* **90**, 1033-45

Kuramitsu, S., Hiromi, K., Hayashi, H., Morino, Y., and Kagamiyama, H. (1990) Pre-steady-state kinetics of *Escherichia coli* aspartate aminotransferase catalyzed

reactions and thermodynamic aspects of its substrate specificity. *Biochemistry* **29**, 5469-5476

Kuramitsu, S., Inoue, K., Ogawa, T., Ogawa, H., and Kagamiyama, H. (1985a) Aromatic amino acid aminotransferase of *Escherichia coli*: Nucleotide sequence of the *tyrB* gene. *Biochem. Biophys. Res. Commun.* **133**, 134-139

Kuramitsu, S., Okuno, S., Ogawa, T., Ogawa, H., and Kagamiyama, H. (1985b) Aspartate aminotransferase of *Escherichia coli*: nucleotide sequence of the *aspC* gene. *J. Biochem (Tokyo)* **97**, 1259-1262

Lamzin, V. S., Dauter, Z., Popov, V. O., Harutyunyan, E. H., and Wilson, K. S. (1994) High resolution structures of holo and apo formate dehydrogenase. *J. Mol. Biol.* **236,** 759-785

Lebioda, L. and Stec, B. (1991) Mechanism of enolase: the crystal structure of enolase-Mg^{2+}-2-phosphoglycerate/phosphoenolpyruvate complex at 2.2-Å resolution. *Biochemistry* **30,** 2817-2822

Malashkevich, V. N., Onuffer, J. J., Kirsch, J. F., and Jansonius, J. N. (1995) Alternating arginine-modulated substrate specificity in an engineered tyrosine aminotransferase. *Nat. Struct. Biol.* **2**, 548-553

Maruta, S., Uyehara, Y., Homma, K., Sugimoto, Y., and Wakabayashi, K. (1999) Formation of the myosin.ADP.gallium fluoride complex and its solution structure by small-angle synchrotron X-ray scattering. *J. Biochem. (Tokyo)* **125**, 177-185

Meador, W. E., Means, A. R., and Quiocho, F. A. (1993) Modulation of calmodulin

plasticity in molecular recognition on the basis of x-ray structures. *Science* **262,** 1718-1721

Mehta, A. D., Rief, M., Spudich, J. A., Smith, D. A., and Simmons, R. M. (1999) Single-molecule biomechanics with optical methods. *Science* **283**, 1689-1695

Miyahara, I., Hirotsu, K., Hayashi, H., and Kagamiyama, H. (1994) X-ray crystallographic study of pyridoxamine 5'-phosphate-type aspartate aminotransferases from *Escherichia coli* in three forms. *J. Biochem (Tokyo)* **116**, 1001-1012

Neuefeind, T., Huber, R., Dasenbrock, H., Prade, L., and Bieseler, B. (1997) Crystal structure of herbicide-detoxifying maize glutathione S-transferase-I in complex with lactoylglutathione: evidence for an induced-fit mechanism. *J. Mol. Biol.* **274**, 446-453

Okamoto, A., Higuchi, T., Hirotsu, K., Kuramitsu, S., and Kagamiyama, H. (1994) X-ray crystallographic study of pyridoxal 5'-phosphate-type aspartate aminotransferases from *Escherichia coli* in open and closed form. *J. Biochem. (Tokyo)* **116**, 95-107

Okamoto, A., Ishii, S., Hirotsu, K., and Kagamiyama, H. (1999) The active site of *Paracoccus denitrificans* aromatic amino acid aminotransferase has contrary properties: flexibility and rigidity. *Biochemistry* **38,** 1176-1184

Olson, A. J., Bricogne, G., and Harrison, S. C. (1983) Structure of tomato busy stunt virus IV. The virus particle at 2.9 Å resolution. *J. Mol. Biol.* **171,** 61-93

O'Reilly, M., Watson, K. A., Schinzel, R., Palm, D., and Johnson, L. N. (1997) Oligosaccharide substrate binding in *Escherichia coli* maltodextrin phosphorylase. *Nat. Struct. Biol.* **4**, 405-412

Otwinowski, Z. (1993) In *CCP4 study weekend data collection and processing* (eds Sawyer, L., Isaacs, N. and Bailey, S.) 56-62 (SERC Daresbury Laboratory, UK)

Oue, S., Okamoto, A., Nakai, Y., Nakahira, M., Shibatani, T., Hayashi, H., and Kagamiyama, H. (1997) *Paracoccus denitrificans* aromatic amino acid aminotransferase: a model enzyme for the study of dual substrate recognition mechanism. *J. Biochem. (Tokyo)* **121,** 161-171

Oue, S., Okamoto, A., Yano, T., and Kagamiyama, H. (1999) Redesigning the substrate specificity of an enzyme by cumulative effects of the mutations of non-active site residues. *J. Biol. Chem.* **274,** 2344-2349

Pai, E. F., Krengel, U., Petsko, G. A., Goody, R. S., Kabsch, W., and Wittinghofer, A. (1990) Refined crystal structure of the triphosphate conformation of H-ras p21 at 1.35 Å resolution: implications for the mechanism of GTP hydrolysis. *EMBO J.* **9,** 2351-2359

Pfister, K., Sandmeier, E., Berchtold, W., and Christen, P. (1985) Conformational changes in aspartate aminotransferase. Effect of active site ligands on peptide hydrogen-deuterium exchange. *J. Biol. Chem.* **260**, 11414-11421

Pugmire, M. J., Cook, W. J., Jasanoff, A., Walter, M. R., and Ealick, S. E. (1998) Structural and theoretical studies suggest domain movement produces an active

conformation of thymidine phosphorylase. *J. Mol. Biol.* **281**, 285-299

Radmacher, M., Fritz, M., Hansma, H. G., and Hansma, P. K. (1994) Direct observation of enzyme activity with the atomic force microscope. *Science* **265**, 1577-1579

Remington, S., Wiegand, G., and Huber, R. (1982) Crystallographic refinement and atomic models of two different forms of citrate synthase at 2.7 and 1.7 Å resolution. *J. Mol. Biol.* **158,** 111-152

Rhee, S., Miles, E. W., and Davies, D. R. (1998) Cryo-crystallography of a true substrate, indole-3-glycerol phosphate, bound to a mutant (alphaD60N) tryptophan synthase alpha2beta2 complex reveals the correct orientation of active site alphaGlu49. *J. Biol. Chem.* **273**, 8553-8555

Rhee, S., Silva, M. M., Hyde, C.C., Rogers, P. H., Metzler, C. M., Metzler, D. E., and Arnone, A. (1997) Refinement and comparisons of the crystal structures of pig cytosolic aspartate aminotransferase and its complex with 2-methylaspartate. *J. Biol. Chem.* **272**, 17293-17302

Rini, J. M., Schulze-Gahmen, U., and Wilson, I. A. (1992) Structural evidence for induced fit as a mechanism for antibody-antigen recognition. *Science* **255,** 959-965

Ryu, K. and Dordick, J.S. (1992) How do organic solvents affect peroxidase structure and function? *Biochemistry* **31,** 2588-2598

Smith, D. L., Almo, S. C., Toney, M. D., and Ringe, D. (1989) 2.8-Å-resolution

crystal structure of an active-site mutant of aspartate aminotransferase from *Escherichia coli.* *Biochemistry* **28,** 8161-8167

Stuckey, J. A., Schubert, H. L., Fauman, E. B., Zhang, Z. Y., Dixon, J. E., and Saper, M. A. (1994) Crystal structure of Yersinia protein tyrosine phosphatase at 2.5 Å and the complex with tungstate. *Nature* **370,** 571-575

Wangikar, P. P., Rich, J. O., Clark, D. S., and Dordick, J. S. (1995) Probing enzymic transition state hydrophobicities. *Biochemistry* **34,** 12302-12310

Wierenga, R. K., Noble, M. E., Postma, J. P., Groendijk, H., Kalk, K. H., Hol, W. G., and Opperdoes, F. R. (1991) The crystal structure of the "open" and the "closed" conformation of the flexible loop of trypanosomal triosephosphate isomerase. *Proteins* **10,** 33-49

Xu, W., Harrison, S. C., and Eck, M. J. (1997) Three-dimensional structure of the tyrosine kinase c-Src. *Nature* **385,** 595-602

Acknowledgments

I would like to express great appreciation to Professor Seiki Kuramitsu for giving me the opportunity to gain more insight into the fascinating fields of biochemistry, for continuing guidance and many valuable discussions, and his helpful advice on the preparation of this manuscript. I gratefully acknowledge the invaluable discussions and supports of Dr. Shin-ichi Kawaguchi, Dr. Ryuichi Kato, and Dr. Ryouji Masui during the course of my study.

I am sincerely grateful to Professor Ken Hirotsu, Dr. Ikuko Miyahara, Dr. Tadashi Nakai (Osaka City University) for teaching me X-ray crystallographic analysis. Special thanks are due to Dr. Mitsuaki Sugahara for his helpful advice on the study of crystallography, to Dr. Tetsuro Fujisawa (Riken) for measurement of X-ray small angle scattering, and to Miss Noriko Nakagawa for valuable discussions.

Finally, I think my colleagues of Professor Kuramitsu's laboratory for their valuable supports.